

TRAPPED SLENDER VORTEX FILAMENTS IN STATISTICAL EQUILIBRIUM

By

Timothy D. Andersen

A Thesis Submitted to the Graduate
Faculty of Rensselaer Polytechnic Institute
in Partial Fulfillment of the
Requirements for the Degree of
DOCTOR OF PHILOSOPHY
Major Subject: Mathematical Sciences

Approved by the
Examining Committee:

Chjan C. Lim, Thesis Adviser

Mark Holmes, Member

Peter Kramer, Member

James Napolitano, Member

Rensselaer Polytechnic Institute
Troy, New York

May 2007
(For Graduation August 2007)

TRAPPED SLENDER VORTEX FILAMENTS IN STATISTICAL EQUILIBRIUM

By

Timothy D. Andersen

An Abstract of a Thesis Submitted to the Graduate

Faculty of Rensselaer Polytechnic Institute

in Partial Fulfillment of the

Requirements for the Degree of

DOCTOR OF PHILOSOPHY

Major Subject: Mathematical Sciences

The original of the complete thesis is on file
in the Rensselaer Polytechnic Institute Library

Examining Committee:

Chjan C. Lim, Thesis Adviser

Mark Holmes, Member

Peter Kramer, Member

James Napolitano, Member

Rensselaer Polytechnic Institute
Troy, New York

May 2007
(For Graduation August 2007)

© Copyright 2007
by
Timothy D. Andersen
All Rights Reserved

CONTENTS

LIST OF FIGURES	iv
ACKNOWLEDGMENT	vi
ABSTRACT	vii
1. Introduction	1
2. Problem and Background	9
2.1 Neutral Fluids	9
2.2 Charged Fluids	12
3. Model	15
4. Canonical Free Energy	20
4.1 Free Energy of Most-Probable Macrostate	20
4.2 Mean Field Assumption	21
4.3 Spherical Constraint	23
4.4 Free Energy Derivation for Radius	24
5. Monte Carlo	30
5.1 Algorithm	30
5.2 Simulation Results	31
5.2.1 Comparison	31
5.2.2 Straightness Holds	33
6. Microcanonical Ensembles	35
7. Discussion and Conclusions	43
7.1 Discussion	43
7.2 Conclusion	44
APPENDICES	
A. Evaluating the Free Energy Integral	49
B. Source Code	50

LIST OF FIGURES

1.1	Shown here in top-down projection, nearly parallel vortex filaments, at low density and high strength of interaction, are well-ordered into a 2-D triangular lattice known as the Abrikosov lattice from type-II superconductors (Abrikosov [1957]). This figure shows how the quasi-2D model is essentially a 2-D model for these parameters.	3
1.2	Nearly parallel vortex filaments are nearly parallel to the z-axis in an asymptotic sense that their deviation from straight is a small parameter. They are infinite in length but have a period L . Here there are 50 filaments.	4
1.3	We assume that a filament interacts with the other filaments as its center-of-mass interacts with the center-of-mass of the rest of the $N - 1$ filaments.	7
5.1	The bisection algorithm works by bisecting the filament to sample point positions. First the center point is selected, then the two points half-way from the center to the end-points, then four more points, eight, and so on until some maximum number of points are sampled. These are snapshots of one filament at different steps in the sampling process.	32
5.2	The mean square vortex position, defined in Equation 5.3, compared with Equations 4.32 and 2.10 shows how 3-D effects come into play around $\beta = 0.16$. That the 2D formula continues to decrease while the Monte Carlo and the quasi-2D formula curve upwards with decreasing β suggests that the internal variations of the vortex lines have a significant effect on the probability distribution of vortices.	33
5.3	This figure shows the mean slope per segment, δ/a , where $\delta \sim 0.0098$ and a is given by Equation 5.4, and that straightness holds for all β values. The point at which R^2 begins to increase with decreasing β (Figure 5.2) has a mean slope of 35, and, even at the smallest $\beta = 10^{-3}$, the segments have an average angle of 82° with respect to the complex plane.	34
6.1	The specific heat at constant pressure (Equation 6.31) for the thermally isolated system is negative, meaning that the constant pressure Enthalpy Per Length (Equation 6.29) decreases with increasing temperature. (Here $\alpha' = 5 \times 10^5$ and $p' = 8 \times 10^4$.)	41

6.2 The Mean Square Vortex Position (Equation 6.12) increases exponentially at high temperature, while it is nearly constant at low-temperature. (Here $\alpha = 5 \times 10^5$ and $p = 8 \times 10^4$.) 42

ACKNOWLEDGMENT

I would like to thank my advisor Chjan C. Lim for the wonderful discussions which led to this thesis and for letting me follow my own path. Thanks also to my committee members for their support and for giving me the benefits of their knowledge. I would like to thank Dr. Chris Arney of ARO and Dr. Anil Deane of DOE for their generous support. This work is supported by ARO grant W911NF-05-1-0001 and DOE grant DE-FG02-04ER25616.

ABSTRACT

The statistical mechanics of nearly parallel vortex filaments confined in the unbounded plane by angular momentum, first studied by Lions and Majda (2000), is investigated using a mean-field approximation to interaction and a spherical constraint to develop an explicit formula for the mean square vortex position or length scale of the system, R , verified with Path Integral Monte Carlo simulations. In addition we study the previously unstudied microcanonical distribution for this system with applications to plasmas. We confirm that 3D filaments resist confinement in a different way than 2D point vortices and that this results in a profound shift at high-densities for the length scale of quasi-2D versus strictly-2D models of vorticity fields in which angular momentum is conserved. Our analytical results correspond well with those of the Monte Carlo simulations and show a 3D effects contributing significantly to determination of the length scale and to transitions to turbulence at high temperature. We also find negative specific heat in the case of the electron magnetohydrodynamic (EMH) plasma model, a rare phenomenon found in gravothermal collapse of globular clusters. This find has implications for magnetic nuclear fusion where compression is crucial to a self-sustaining nuclear reaction.

CHAPTER 1

Introduction

Statistical mechanics is a way of calculating the macroscopic properties of matter from the probabilistic behavior of its microscopic components. Rather than solving the Navier-Stokes equations explicitly in time, a statistical equilibrium approach for fluid flows aims to describe observable quantities by averaging over “microstates” or states that account for a system’s exact position in phase space.

In fluid turbulence a statistical treatment is often preferable to obtaining direct solutions to the Navier-Stokes equations because of the inherent chaos/complexity of turbulent flows that makes it impossible to model every trajectory at high Reynolds numbers. This nonequilibrium statistical description of turbulence can be replaced by a statistical equilibrium approach under specific conditions such as nearly inviscid quasi-2D flows where a separation of time scales is valid. Familiar arguments in favor of a separation in the time scales of energy and angular momentum transfer at flow boundaries versus viscous dissipation are based on the tea cup paradigm. The “universal equilibrium assumption”, that the time scale at which turbulent features form is much smaller than the time scale for viscous decay, justifies studying turbulent flows in equilibrium (Chorin [1994]). Although this justification can be considered tenuous and subject to mathematical limits, experimental observations provide a validation for the statistical approach.

Most work on fluid flows in statistical equilibrium is on how large scale structures appear in vorticity fields of 2D rotating ideal fluids such as Onsager’s Point Vortex Gas (Onsager [1949]). Many significant results have come out of this approach, but research has confirmed few 2D results for nearly-2D or quasi-2D models. In many cases, 2D models approximate a quasi-2D reality. This thesis is concerned with when this approximation fails and how the statistics of quasi-2D models depart from those of fully-2D when it does fail.

Applications of these quasi-2D models are relevant to geophysical and astrophysical flows at scales where Coriolis effect is negligible and to magnetohydrody-

namics of charged fluids in plasmas. Although the statistics of geo/astrophysical flows and plasmas are different, there are at least two direct translation between the Euler equations for ordinary fluids and the equations governing plasmas. The first is the 2D guiding center plasma (Joyce and Montgomery [1973], Edwards and Taylor [1974], Fine et al. [1973]). Because the Coulomb interaction and the vortex interaction are identical, point vortex dynamics automatically applies to guiding center plasmas. However, quasi-2D models are more appropriately applied to the electron magnetohydrodynamical model (EMH) where the magnetic flux and the motion of electrons, connected via Ampere's law, can combine into a single vorticity description identical to that of ordinary fluid vortex models (Uby et al. [1995]).

Nearly parallel vortex filaments (Figure 1.2) is one of the simplest models for discrete, quasi-2D vorticity. They appear in an incompressible, nearly inviscid Navier-Stokes flow (Klein et al. [1995]) as well as other physical systems such as in rotating superfluids and Bose-Einstein condensates. From theories for single vortex filaments by Hasimoto [1972], Callegari and Ting [1978], Ting and Klein [1991], and Klein and Majda [1991], Klein, Majda and Damodaran (Klein et al. [1995]) developed the first rigorous model for *interacting* nearly parallel filaments. Julien et al. [1996] have observed these nearly parallel vortex filaments in astrophysical simulations.

Our statistical description of nearly parallel vortex filaments, as presented in our papers, (Andersen and Lim [2007a], Andersen and Lim [2007b]), derives from the work of Lions and Majda [2000]. In their paper, they developed a description of the time-dependent statistics, namely the density, $\rho(t, \mathbf{r})$, where $\mathbf{r} \in \mathfrak{R}^2$, of the filaments for $N \rightarrow \infty$, given that energy and angular momentum are conserved, using the model of Klein et al. [1995]. Filaments are also periodic in the z-direction with period L , and, as in the related statistical derivations of Berdichevsky [1998], filaments are smooth.

They introduce a Gibbs probability measure for the vortex filaments in the unbounded plane, confined by angular momentum. This distribution models a system that is not completely isolated, a reasonable assumption in geophysical and other macroscopic flows, in that a quiescent fluid surrounding the filaments acts as

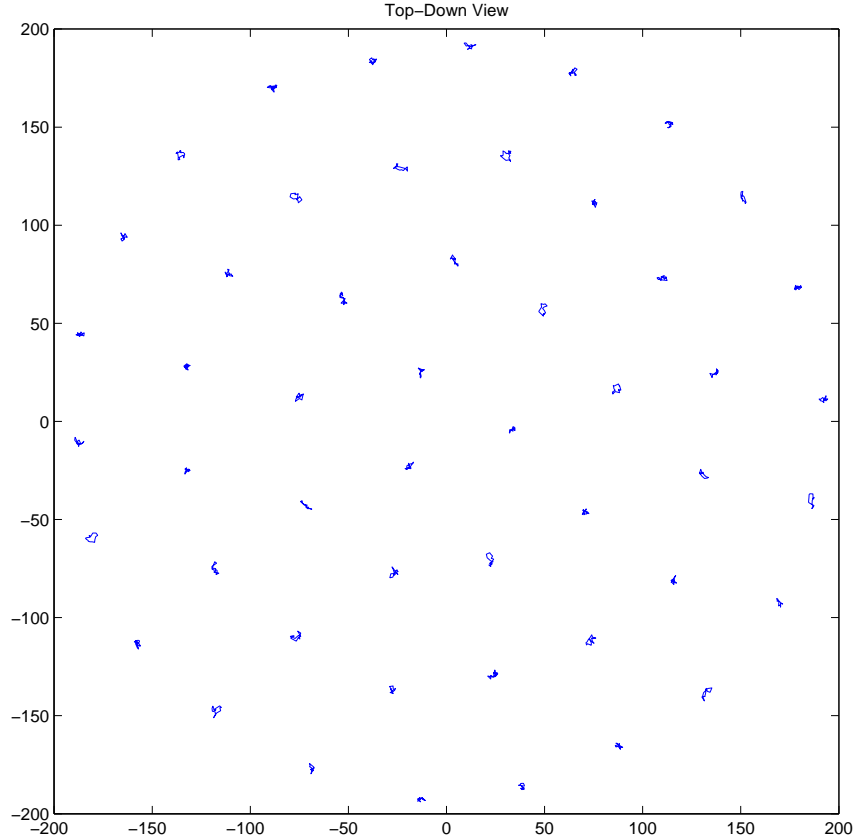


Figure 1.1: Shown here in top-down projection, nearly parallel vortex filaments, at low density and high strength of interaction, are well-ordered into a 2-D triangular lattice known as the Abrikosov lattice from type-II superconductors (Abrikosov [1957]). This figure shows how the quasi-2D model is essentially a 2-D model for these parameters.

an energy and angular momentum bath. The system is allowed to exchange angular momentum and energy with the environment and so angular momentum and energy fluctuate. A justification, *a posteriori*, of the Gibbs' probability measure that is canonical, rather than microcanonical, in energy and angular momentum comes from results indicating that vortices are confined to a compact domain in the plane, and the heat bath exists outside this domain.

In formal notation, a canonical ensemble (CE) Gibbs' measure means that if

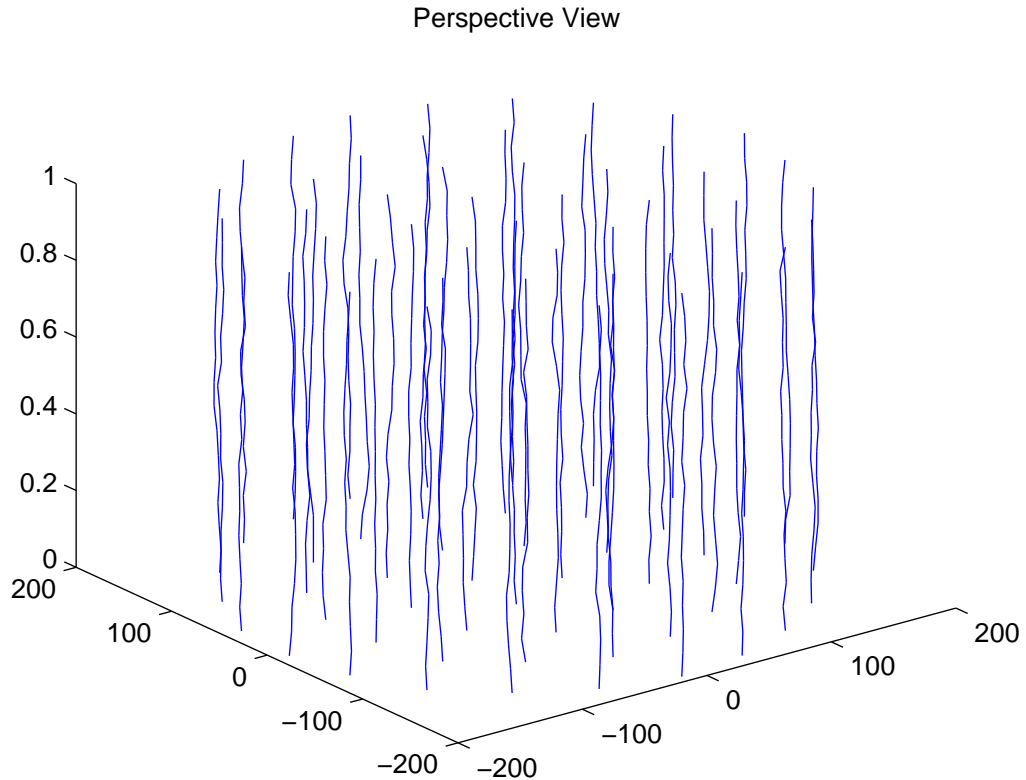


Figure 1.2: Nearly parallel vortex filaments are nearly parallel to the z -axis in an asymptotic sense that their deviation from straight is a small parameter. They are infinite in length but have a period L . Here there are 50 filaments.

a state s has energy E_s and angular momentum I_s , then the probability of s ,

$$P_{\text{CE}}(s) \propto e^{-\beta E_s - \mu I_s}, \quad (1.1)$$

where β and μ are constants. (For historical reasons β is known as inverse “temperature” and μ as “chemical potential” although they are not directly related to their molecular equivalents because the “molecules” here are vortices.) Since $\sum_s P_{\text{CE}}(s) = 1$, $P_{\text{CE}}(s) = Z_{\text{CE}}^{-1} e^{-\beta E_s - \mu I_s}$, where $Z_{\text{CE}} = \sum_s e^{-\beta E_s - \mu I_s}$ (Chorin [1994]). Lions’ and Majda’s rigorous treatment of this statistical ensemble leads to a non-linear Schroedinger equation governing ρ . Their approach has been criticized as being physically inconsistent because it admits states that are not nearly parallel

(Berdichevsky [2002]). This criticism is valid. However, a careful choice of parameters β , μ , etc. causes these disallowed states to have such large energies that their probabilities are negligible. For such parameter ranges, we can assume that the Lions-Majda model is physical. Our Monte Carlo simulation naturally rejects states with non-nearly-parallel lines without additions to the model.

In our papers, (Andersen and Lim [2007c], Andersen and Lim [2007d]), we address the electron magnetohydrodynamical (EMH) model for plasmas (Uby et al. [1995]) under strong, stable external confinement. Here we reproduce those results. The EMH model bypasses the complexities of the two-fluid, magnetohydrodynamical model by representing the strongly confined, charged fluid and the magnetic field as a single, generalized fluid with a neutralizing ion background. This model takes the magnetic field, $\mathbf{B} = \nabla \times \mathbf{A}$, and the charged fluid vorticity, $\omega = \nabla \times \mathbf{v}$, and combines them into a general vorticity field $\Omega = \nabla \times \mathbf{p}$ where the generalized momentum, $\mathbf{p} = m\mathbf{v} - e\mathbf{A}$, m is the electron mass, $-e$ is the electron charge, \mathbf{v} is the fluid velocity field, and \mathbf{A} is the magnetic vector potential field. The flow field of such a vorticity model indicates electrons are swirling around magnetic flux lines. Since magnetically confined plasmas should be energetically isolated, the correct model is a microcanonical ensemble (MCE) in enthalpy:

$$P_{\text{MCE}}(s) = Z_{\text{MCE}}^{-1} \delta(NH_0 - E_s - pI_s) \delta(I_0 - I_s), \quad (1.2)$$

where H_0 is the total enthalpy per vortex per period of the plasma, I_0 is total angular momentum per vortex per period, $Z_{\text{MCE}} = \int ds \delta(NH_0 - E_s - pI_s) \delta(NR^2 - I_s)$, p is the pressure, and $s = \{\psi_1, \dots, \psi_N\}$. The magnetic confinement is stronger than the induced magnetic field. The term *enthalpy* is used here loosely to refer to $E_s + pI_s$. Normally in a gas, enthalpy refers to $E + pV$ where E is energy p is pressure and V is volume. In our case the ‘‘volume’’ is angular momentum, I_s , which is proportional to the actual volume of the system. Energy is still energy, E_s , and ‘‘pressure’’, p , is the multiplier to the angular momentum.

The conservation of 2D angular momentum is key in this study because it introduces a natural length scale to the confined system of filaments in the unbounded plane (DiBattista and Majda [2001]). It also plays an important role in statistical

mechanics on the sphere (Lim and Nebus [2006], Lim [2006]). Periodic boundary conditions are more common, but these enforce a length scale (the period) artificially on the plane that can affect the statistics. Although a pre-determined length scale is reasonable in some cases, for many others, it is not. Moreover, the statistics for periodically bounded ensembles is quite different from unbounded systems that are confined by angular momentum or a harmonic trap as in the case of Bose-Einstein condensates. As the reader will see in this paper, our results, which focus on determining the length scale both analytically and computationally, depend upon the angular momentum confinement. The conservation of 2D angular momentum, is of course, unnatural in a 3D world and suggests a symmetry breaking process such as a strong magnetic field in the case of the EMH model or convection currents in the case of geophysics. We do not address the details of such forcing processes in our equations but assume their existence.

Our goal is not merely to demonstrate that nearly parallel vortex filaments behave differently from 2D point vortices. Nearly parallel vortex filaments at low-density/high-straightness (large β or low-temperature) behave *exactly* like 2-D point vortices (Figure 1.1). That their behavior at high densities and levels of curvature (small β or high-temperature) ought to be different than that of 2D point vortices is obvious. On the other hand, despite the rigorous work of Lions and Majda, the qualitative statistical differences between nearly parallel vortex filaments and strictly-parallel filaments or 2D point vortices are unknown, and, in the plasma case, no work has been done.

Our hypothesis is that at high-densities point vortices and nearly parallel vortex filaments have qualitatively different behavior. The length scale of point vortices collapses with increasing temperature (Lim and Assad [2005]). We hypothesize that filaments reverse this collapse in a way unlike point vortices (Sec. 5.2). Similarly to how stars in globular clusters resist gravitational collapse through motion, we posit that filaments resist collapse through curvature (which in top-down projection appears like Brownian motion) and that the outcome is a reversal of collapse as temperature increases. This idea has profound implications for the natural length scale of 2D versus quasi-2D models and nature of magnetic compression in plasmas.

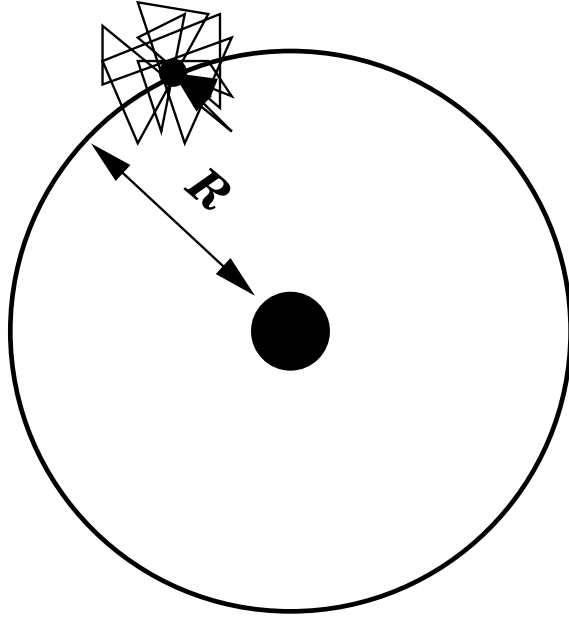


Figure 1.3: We assume that a filament interacts with the other filaments as its center-of-mass interacts with the center-of-mass of the rest of the $N - 1$ filaments.

We develop a simpler approach than Lions and Majda—one that is motivated and justified by their rigorous mean-field result—that we hope generates a more intuitive understanding of what happens when the density and curvature of the filaments increases and interaction becomes more three dimensional. Our method is two-fold:

1. We develop an explicit formula for free energy of the canonical system as a function of the second moment, R^2 , defined in the non-extensive limit $\beta' = \beta N$ and $\alpha' = \alpha/N$, as

$$R^2 = \lim_{N \rightarrow \infty} \int ds \frac{1}{N} \sum_i L^{-1} \int_0^L d\tau |\psi_i(\tau)|^2 P_{\text{CE}}(E_s, I_s), \quad (1.3)$$

where $s = (\psi_1, \dots, \psi_N)$, α is core-structure related to core velocity. (We show that R^2 is the same in either the canonical or microcanonical case in the non-extensive limit.) We introduce a simpler mean-field approximation to interaction than Lions-Majda. Our mean-field approach assumes that the interaction due to $N - 1$ filaments on one filament is similar to how a perfectly

straight filament fixed at the origin with strength $N - 1$ would affect the the center-of-mass of that filament (Figure 1.3). This assumption requires that the filaments be fairly uniformly distributed, whereas Lions-Majda do not require uniformity. It is a “center-of-mass interacting with a center-of-mass” rather than “particle interacting with a density field” assumption. We then constrain the filament’s planar position such that,

$$\int_0^L d\tau |\Psi(\tau)|^2 = LR^2, \quad (1.4)$$

where $\Psi(\tau) = x(\tau) + iy(\tau)$ represents the curve of a filament in complex notation. This constraint enters the Gibbs distribution (Eqn. 1.1) as an exact (microcanonical) conservation law. These two assumptions, discussed in detail below, allow us to derive a formula in the non-extensive limit for the minimal Gibbs free energy of the canonical system. In the microcanonical system, this microcanonical constraint is exact rather than approximate, and we use it to maximize the entropy of the system.

2. To confirm our formulas, we perform Path Integral Monte Carlo (Ceperley [1995]) on the canonical distribution using piecewise linear approximations to the filaments. These simulations also allow us to determine that our results are physical, addressing the point of criticism by Berdichevsky [2002]. (Section 5.1.)

Our statistical derivation not only answers the questions above but gives an extremely close prediction of length scale, R , and allows us to explain the qualitative differences between a strictly-2D and a nearly-2D model, giving new insight into the role of 3D effects in the onset of turbulence in quasi-2D models. Furthermore, in the microcanonical case, we derive a negative specific heat, a rare phenomenon found in gravo-thermal collapse of globular clusters (Lynden-Bell and Wood [1968]), that has profound implications for magnetic nuclear fusion research where it is crucial to a self-sustaining reaction.

CHAPTER 2

Problem and Background

Understanding vorticity in geo/astrophysical flows and in electron plasmas with neutralizing background are two separate problems with same Hamiltonian formulation. In geo/astrophysics we would like to know something about the length scales of rotating currents, how energy, temperature, and angular momentum determine their size and other statistical properties. For plasmas we are interested in confinement of the charged fluid of electrons on a short time scale where the ions can be considered a constant substrate. The specific heat is an especially important statistical property.

2.1 Neutral Fluids

One of the main purposes of this investigation is to describe the specific differences between quasi-2D and 2D models of vorticity, i.e. when and how 3D effects influence the planar statistical distribution of vortices.

Consider a fluid with velocity vector $\mathbf{u}(\mathbf{r}) \in \mathbb{R}^3$ where \mathbf{r} is a position in 3-space. The incompressible, $\nabla \cdot \mathbf{u} = 0$, Navier-Stokes equation describes the behavior of vorticity, $\omega = \nabla \times \mathbf{u}$,

$$\frac{D\omega(\mathbf{r})}{Dt} = (\omega \cdot \nabla)\mathbf{u} + \text{Re}^{-1}\Delta\omega \quad (2.1)$$

where $D \cdot /Dt = \partial_t + \mathbf{u} \cdot \nabla$ is total derivative and Re is the Reynolds number. In the case of 2D motion the equation reduces to

$$\frac{D\omega(x, y)}{Dt} = \text{Re}^{-1}\Delta\omega, \quad (2.2)$$

and for the inviscid case, $D\omega/Dt = 0$ (Chorin [1994]).

If we break the 2D vorticity into points of fixed strength, such that,

$$\omega(x, y) = \sum_{i=1}^N \lambda_i \delta(x - x_i) \delta(y - y_i), \quad (2.3)$$

then the system is a finite Hamiltonian one,

$$\lambda_i \frac{\partial x_i}{\partial t} = \frac{\partial H_N^{2D}}{\partial y_i} \quad \lambda_i \frac{\partial y_i}{\partial t} = -\frac{\partial H_N^{2D}}{\partial x_i} \quad (2.4)$$

where

$$H_N^{2D} = -\frac{1}{2} \sum_{j>i} \lambda_i \lambda_j \log |z_i - z_j|^2, \quad (2.5)$$

where λ_i and λ_j are the circulation constants for point vortices i and j , and $z_i = x_i + iy_i$ and $z_j = x_j + iy_j$ are their positions in the complex plane. (Complex coordinates will be used for the rest of this thesis.)

The canonical probability distribution, appropriate for geo/astrophysical flows where there is surrounding fluid but *not* appropriate for plasmas where there is none,

$$P = \frac{\exp(-\beta H_N - \mu I_N)}{Z}, \quad (2.6)$$

where

$$Z = \int dz_1 \cdots \int dz_N \exp(-\beta H_N^{2D} - \mu I_N^{2D}) \quad (2.7)$$

and

$$I_N^{2D} = \sum_i \lambda_i |z_i|^2, \quad (2.8)$$

represents a non-isolated system in which energy and angular momentum are conserved but exchanged with the environment at some level of fluctuation determined by the “inverse temperature”, β , and the “chemical potential”, μ .

This system has been studied extensively since Onsager [1949] showed negative temperature states $\beta < 0$ and decades later Joyce and Montgomery [1973], Edwards and Taylor [1974] carried it over to guiding center plasma models. Even in 2D magnetohydrodynamics this model applies (Kinney et al. [1993]). The underlying assumption for studying such models is that there are many processes, such

as convection currents and polarizing external magnetic fields, that break the 3D symmetry of fluids so that they behave like 2D fluids. Even something as simple as stirring tea in a cup can create a 2D fluid, albeit for only a few seconds without forcing.

Two-dimensional and three-dimensional fluids have significant, qualitative differences in behavior. As Kolmogorov [1941] showed, even before Onsager, in 3D fluids the majority of the energy cascades down to smaller and smaller order while in 2D fluids most of it cascades up to larger-scale order. Therefore, the interest in 2D fluids is in the appearance of this large-scale order. The extended interest in quasi-2D fluids, then, is to see when and how this large-scale order changes qualitatively with 3D effects.

In their paper, Lim and Assad [2005] show variationally that the mean square vortex position (variance) for 2D point vortices in the non-extensive limit, $\beta' = N\beta$,

$$R_{2D}^2 = \lim_{N \rightarrow \infty} \langle N^{-1} \sum_i |\Psi_i|^2 \rangle, \quad (2.9)$$

where the average is over P , has a nice formula

$$R_{2D}^2 = \frac{\Lambda\beta}{4\mu}, \quad (2.10)$$

where $\Lambda = \sum_i \lambda_i$ is the total circulation. In our case, we define $\lambda_i = 1 \forall i$, so $\Lambda = N$ and $R_{2D}^2 = N\beta/(4\mu) = \beta'/(4\mu)$. Moreover, they were able to show in Monte Carlo simulations of an ensemble of 1000 point vortices that the distribution of vortices is almost uniform and axisymmetric, meaning that the probability distribution of vortices is nearly a perfect cylinder, suggesting that R_{2D}^2 is the only value we need to know to determine the entire distribution.

These results provide a tantalizing starting point for our investigation of nearly parallel vortex filaments where, obviously, at some level of density and fluctuation there exists different statistical behavior. Moreover, the discovery of a uniform distribution at low-temperature, we hope, carries over to nearly parallel vortex filaments.

The low-temperature formula for R_{2D}^2 , Equation 2.10, decreases with β , mean-

ing that the radius decreases as the “temperature”, related to the speed of motion of the vortices, increases. At some point, of course, β is so small that the distribution becomes solely a function of angular momentum, clearly a normal distribution with variance, $R_{2D}^2 = 1/(2\mu)$. The radius does not decrease to a point, but it *never* increases, certainly not in the low-temperature regime.

The question with respect to neutral fluids that we address in this thesis concerns the statistical distribution of nearly parallel vortex filaments at low to moderate temperature, *not* high-temperature. Therefore, our derivations in Section 4 assume that β is large enough that the *fluctuations* in interaction energy and angular momentum do not play a major role in the statistics, only their mean-values. The role of the Monte Carlo comparison in Section 5.2 is to justify this assumption. Specifically, we are concerned with the mean square vortex position, R^2 , defined in Equation 1.3 and the Gibbs free energy which will indicate if any phase transitions occur.

2.2 Charged Fluids

Magnetohydrodynamics (MHD) for plasmas is normally a two fluid model because ions and electrons must be treated separately. However, at short time scales the ions can be considered to be a neutralizing background substrate and unmoving, collisions between electrons and ions can also be ignored. We briefly discuss the EMH model here. For detailed accounts, see Kingsep et al. [1989], Gordeev et al. [1994]. The equations of motion are

$$m \left[\frac{\partial \mathbf{u}}{\partial t} + \mathbf{u} \cdot \nabla \mathbf{u} \right] = -\frac{\nabla P}{n} - e(\mathbf{E} + \mathbf{v} \times \mathbf{B}), \quad (2.11)$$

where m and $-e$ are electron mass and charge, \mathbf{u} is velocity, n , number density, and P pressure. The model assumes that the electron displacement current is negligible, charge density is uniform. (The electric field does not change appreciably on this time scale.) The magnetic field then has from Ampère’s Law:

$$\nabla \times \mathbf{B} = -\mu_0 e n \mathbf{u}, \quad (2.12)$$

and Faraday's law, $\nabla \times \mathbf{E} = -\partial\mathbf{B}/\partial t$, defines the electric field. Taking the curl of Equation 2.11 and applying Equation 2.12 gives the so-called “frozen field” equation,

$$\frac{\partial\Omega}{\partial t} = \nabla \times (\mathbf{u} \times \Omega), \quad (2.13)$$

where

$$\Omega = \nabla \times \mathbf{p}, \quad \mathbf{p} = m\mathbf{u} - e\mathbf{A}. \quad (2.14)$$

Interestingly, vorticity in ordinary, inviscid, incompressible hydrodynamics also satisfies the frozen-field equation (Hornig [2003]). In the next chapter we will make use of this connection and give a justification for it.

In a study of plasmas in a toroidal geometry appropriate to a Tokamak, Kiessling and Neukirch [2003] have found negative specific heat in the microcanonical ensemble using variational principle on the strictly-parallel, density model for guiding center plasmas. Therefore, we have reason to think that the nearly parallel model for generalized vorticity also has negative specific heat in the periodic (toroidal for a large toroid with a comparatively small cross-section where curvature is negligible).

Schrödinger, in his book (Schrödinger [1952]), gave a “proof” that a system with canonical conservation of energy, specific heat must be positive. Consider a canonical ensemble where average enthalpy is,

$$\langle E \rangle = \frac{\sum_i E_i \exp(-\beta E_i)}{\sum_i \exp(-\beta E_i)}, \quad (2.15)$$

then the specific heat

$$C_p = \frac{d\langle E \rangle}{dT} = -k_B \beta^2 \frac{d\langle E \rangle}{d\beta} = k_B \beta \langle (E_i - \langle E \rangle)^2 \rangle, \quad (2.16)$$

is clearly positive.

However, in the microcanonical setting, specific heat can be negative. With a positive specific heat system, isolated systems can be multiplied and one considered in a heat bath in equilibrium. This indicates that microcanonical and canonical systems with positive specific heat are equivalent because they are *extensive*. Thirring

[1970] pointed out that a system with negative specific heat cannot be in thermal equilibrium in the presence of a heat bath, so negative specific heat systems are *non-extensive*. Two negative specific heat systems in contact with one another will cause one to become hotter as it loses energy and the other to grow colder as it gains energy. Because the two systems have opposite behavior, there is no equilibrium. Negative specific heat is often found in systems with binding energy that increases as the square of the number of particles, i.e. long-range binding energy such as the logarithmic Coulomb interaction.

For globular clusters, the specific heat dips from positive to negative as a function of E in the microcanonical setting, then in the corresponding canonical setting one expects a phase transition and positive specific heat (Lynden-Bell and Lynden-Bell [1977]). However, even without a phase transition, negative specific heat is and rare and profound find because, in the non-equilibrium setting, it indicates a runaway reaction to collapse of the system.

CHAPTER 3

Model

The nearly parallel vortex filament model that we use for both the EMH and geophysical arenas is derived through an asymptotic matching procedure pioneered by Callegari and Ting [1978], Ting and Klein [1991], Klein and Majda [1991] for individual filaments of vorticity.

Vortex filaments (whether nearly parallel or not) influence the fluid around them via the Biot-Savart law. Let us assume a quiescent fluid with no background flow field. Take a filament parameterized by $\mathbf{X}(\tau, t) \in \mathbb{R}^3$. The velocity, \mathbf{u} , a vortex filament with circulation λ induces on a point $\mathbf{P} = (x, y, z)$ in the surrounding fluid is:

$$\mathbf{u}(\mathbf{P}, t) = -\frac{\lambda}{4\pi} \int \frac{[\mathbf{P} - \mathbf{X}(\tau', t)] \times d\tau'}{[\mathbf{P} - \mathbf{X}(\tau', t)]^3}. \quad (3.1)$$

Inside the core of the filament, the Navier-Stokes evolution equation,

$$\frac{D\mathbf{u}(\mathbf{P})}{Dt} = -\nabla p + \text{Re}^{-1} \Delta \mathbf{u}, \quad (3.2)$$

induces the velocity, where p is pressure. Asymptotic matching seeks to derive the equations of motion of the filament by matching Navier-Stokes core velocity and Biot-Savart induced velocity on a single point, \mathbf{P} , close to the central line, $\mathbf{X}(\tau, t)$, of the vortex, i.e. $\mathbf{P} = r\hat{r} + \mathbf{X}$ as $r \rightarrow 0$, where \hat{r} is a unit radial vector such that $\hat{r} \cdot \hat{t} = 0$ where $\hat{t} = \mathbf{X}'/|\mathbf{X}'|$. This lengthy procedure produces the equations of motion of the asymptotically thin vortex.

We define nearly parallel vortex filaments.

Definition 3.0.1. *Nearly parallel vortex filaments are smooth curves with a complex parameterization $\psi_i(\tau)$ where $\psi_i(\tau, t) = x_i(\tau, t) + iy_i(\tau, t)$ and $\tau \in [0, L]$ where t is time. Given that $L \in O(1)$, if we take any two values of τ , τ_0 and τ_1 such that $\tau_0 < \tau_1$, and let $\Delta\tau = \tau_1 - \tau_0$ such that $\Delta\tau \in O(\epsilon)$ where $\epsilon \ll 1$, then for any filament i , the amplitude $|\psi_i(\tau_1) - \psi_i(\tau_0)| \in O(\epsilon^2)$.*

In words this means that, for a small rise of length ϵ in the filament, the

amplitude must be on the order of ϵ^2 . This assumption guarantees a certain degree of straightness in the filament that allows for the derivation of the quasi-2D equations of motion. The other asymptotic assumption is of the vortex core-size, h , which has the property $h \ll \epsilon$. In this model we assume that the vortices have no cross-section, i.e. the vorticity field, ω , has the form,

$$\omega(\mathbf{r}, t) = \sum_i \int d\tau \delta(\mathbf{r} - \mathbf{r}_i(\tau)). \quad (3.3)$$

where $\mathbf{r}_i = (x_i, y_i, \tau)$ is the position of the filament.

Klein, Majda, and Damodaran (KMD) (Klein et al. [1995]) showed that a collection of filaments with the above nearly parallel asymptotic representation obey the system of PDEs:

$$-i \frac{\partial \psi_i}{\partial t} = \frac{\partial^2 \psi_i}{\partial \tau^2} + 2 \frac{\psi_i - \psi_j}{|\psi_i - \psi_j|^2}, \quad (3.4)$$

a nonlinear Schroedinger equation as $\epsilon \rightarrow 0$. The small parameter ϵ satisfies,

$$h \ll \epsilon^2 \ll 1, \quad (3.5)$$

where h is the vortex core width. Before their rigorous approach to multiple interacting filaments, this PDE had been obtained heuristically by adding together the diffusion (first) term from derivations for individual, nearly straight filaments and the interaction (second) term from perfectly straight filaments.

Our model properly derives from the paper of Lions and Majda [2000] and the Gibbs distribution that they introduce. Although Klein et al. [1995] derived the equations of motion, we make use of the statistical framework presented in the later paper and also we rely heavily on their broken-segment model, not only in the Monte Carlo simulation where it is necessary to discretize the z-axis but also in our mean-field approach.

Equilibrium statistical mechanics is traditionally concerned with conserved quantities in a Hamiltonian system. The Hamiltonian Klein et al. [1995] derived for

nearly parallel vortex filaments has the form,

$$H_N = \alpha \int_0^L d\tau \sum_{i=1}^N \frac{1}{2} \left| \frac{\partial \psi_i(\tau)}{\partial \tau} \right|^2 - \int_0^L d\tau \sum_{i=1}^N \sum_{j>i}^N \log |\psi_i(\tau) - \psi_j(\tau)|, \quad (3.6)$$

where α is the core-structure constant in units of energy/length. This Hamiltonian resembles the 2D point vortex Hamiltonian in that the interaction is logarithmic in the plane. For two filaments i and j , only points in the same plane, the same value of τ , interact. Two points at different values of τ only interact if they are both on the same filament. The first term is a local self-induction term that essentially causes the filaments to wriggle in top-down projection like a particle under Brownian motion. The additional conserved quantity, angular momentum, is given by,

$$I_N = \sum_i \int_0^L d\tau |\psi_i(\tau)|^2. \quad (3.7)$$

Lions and Majda [2000] introduce a broken segment model in Section 2.2, Equation 2.20 of their paper. For each i , $\Psi_i(\tau)$ is piecewise linear with M segments. Each vertex or “bead” is at a multiple of $\delta = L/M$. Therefore, we define $\psi_i(k) = \Psi_i((k-1)\delta)$, and the curve for filament i is given by the vector $\Psi_i = (\psi_i(1), \dots, \psi_i(M))$. With this representation we rewrite the conserved quantities,

$$H_N(M) = \alpha \sum_{i=1}^N \sum_{k=1}^M \frac{1}{2} \frac{|\psi_i(k+1) - \psi_i(k)|^2}{\delta} - \sum_{i=1}^N \sum_{j>i}^N \sum_{k=1}^M \delta \log |\psi_i(k) - \psi_j(k)|, \quad (3.8)$$

$$I_N(M) = \sum_{i=1}^N \sum_{k=1}^M \delta |\psi_i(k)|^2. \quad (3.9)$$

The Gibbs probability measure for a state $s = (\Psi_1, \dots, \Psi_N)$ is then

$$P(s) = Z^{-1} \exp(-\beta H_N(M) - \mu I_N(M)), \quad (3.10)$$

where the partition function has the form,

$$Z_N(M) = \int_{\mathcal{C}^{MN}} d\Psi_1 \cdots d\Psi_N \exp(-\beta H_N(M) - \mu I_N(M)). \quad (3.11)$$

We note that while it is possible to simulate the system with Monte Carlo it is not possible to solve explicitly for Z_N for any value of M . In their paper, Lions and Majda [2000] go on to derive a non-linear Schroedinger equation that can give approximate values for $P(s)$. Their PDE captures a great deal of the statistics, but they do not provide any explicit formula for the length scale R , which is our goal. We refer the reader to their paper to learn more about their derivation and the model.

The Hamiltonian functional for the EMH model is the same as in the ordinary vorticity model because of the Bohr-Van Leeuwen theorem which states that the magnetic field cannot affect the statistics of a classical model. Therefore, only the motion of the electron fluid (an Euler fluid) affects the statistics. The main detail of the proof (which Niels Bohr proved in his 1911 PhD thesis and Van Leeuwen published separately later on (Bohr [1911], Van Leeuwen [1921])), is that given a *classical* Hamiltonian for a number of electrons, M ,

$$H = \sum_i^M \left(\frac{\mathbf{p}_i - e\mathbf{A}_i}{2m} \right)^2 + V(\mathbf{q}_i), \quad (3.12)$$

where \mathbf{p}_i is momentum, \mathbf{A}_i is magnetic vector potential, \mathbf{q}_i is position, then the partition function that determines the statistics is

$$Z = \int d\mathbf{p}_1 \cdots \int d\mathbf{p}_M \int d\mathbf{q}_1 \cdots \int d\mathbf{q}_M \delta(E - H), \quad (3.13)$$

where E is the total system energy. Because the limits on the integrals are infinite, we can replace $\mathbf{p}_i - e\mathbf{A}_i$, with a new momentum, \mathbf{p}'_i , and have exactly the same partition function. Therefore, we can prove from first principles that the magnetic field does not affect the statistics at all. This does not apply to quantum models where the momentum is an operator, but, in our classical fluid model, it proves that the KMD applies directly to the EMH model for plasmas.

The proof is in the definition of the vorticity for the EMH model, $\Omega = \nabla \times \mathbf{p}$, where $\mathbf{p} = m\mathbf{v} - e\mathbf{A}$ is generalized momentum. Given this definition of momentum, the vorticity satisfies the frozen field equation, as mentioned in the previous chapter. The frozen field equation can also be obtained from the incompressible Euler equations from the which the KMD model derives. Therefore, vorticity in both models has the same general behavior. Differences in constants and scales can cause the real systems to behave somewhat differently, but mathematically they are identical. We make no alterations to the Hamiltonian to adapt it to the EMH model. We assume that the quasi-2D structure originates from a polarizing field that keeps the angular momentum absolutely conserved.

CHAPTER 4

Canonical Free Energy

4.1 Free Energy of Most-Probable Macrostate

Given a functional for the free energy for a system, F , it is possible to solve for the statistics of the most-probable macrostate by minimizing F with respect to the desired statistic. In our case the statistic is the second moment of P_1 (Eqn. 1.1), R^2 , defined in Equation 1.3.

The difficulty lies in deriving that functional. In systems such as ours, with variable angular momentum the Gibbs description of free energy is appropriate, $F = U + PV - TS$, where U is average energy, P is pressure, V is volume (proportional to the angular momentum), T is temperature, S is entropy.

In our system we write the free energy as follows:

$$F_N = \langle H_N \rangle + \frac{\mu}{\beta} \langle I_N \rangle - \frac{1}{\beta} S_N, \quad (4.1)$$

where $S = S_N$, $U = \langle H_N \rangle$, $PV = \frac{\mu}{\beta} \langle I_N \rangle$, and $T = \frac{1}{\beta}$.

While many statistical mechanics approaches are devoted to finding a functional for S_N , since H_N and I_N are usually known, there is another way to develop the free energy functional from the partition function Z_N . The function Z_N can be considered a sum over microstates, s_i , or it can be an average over a set of macrostates, σ_j . Equation 2.7 is a sum over microstates. Alternatively, the partition function is given by the formula

$$Z_N = \sum_j \exp(-\beta H_N[\sigma_j] - \mu I_N[\sigma_j]) P[\sigma_j], \quad (4.2)$$

where P is the probability for macrostate σ_j .

Since $S_N[\sigma_j] = \log P[\sigma_j]$, using the formula 4.1, we can say,

$$\begin{aligned} Z_N &= \sum_j \exp(-\beta H_N[\sigma_j] - \mu I_N[\sigma_j] + S[\sigma_j]) \\ &= \sum_j \exp(-\beta F_N[\sigma_j]). \end{aligned} \quad (4.3)$$

Because of conservation laws, we assume in physics that the most-probable macrostate or energy-state, $j = m$, has a probability so much larger than the probabilities of all other macrostates that sum contributions from other macrostates can be neglected and

$$Z_N = \exp(-\beta F_N[\sigma_m]). \quad (4.4)$$

Therefore, we have an equation for the free energy,

$$F_N = -\frac{1}{\beta} \log Z_N. \quad (4.5)$$

Even though this free energy is only the free energy of the most-probable macrostate, it can be considered the system's free energy. Another way to put this is that in the isothermal (fixed β , fixed μ) hypersurface of microstates, the overwhelming majority of the surface area belongs to the most-probable macrostate. (For microcanonical systems we consider the energy level set rather than the temperature one.)

4.2 Mean Field Assumption

As mentioned in Section 3, we cannot solve for Z_N . We need to approximate it to derive the free energy functional. One way to do this is with a mean-field assumption. Because the logarithmic interaction in the Hamiltonian prevents us from evaluating the integral over microstates, Equation 2.7, we need to remove the interdependence of filaments upon one-another so that we can separate the integrals over different filaments. In their paper this is the approach of Lions and Majda [2000], in that they develop a model of a filament that interacts with a probability distribution, or field, rather than other filaments. Our approach is to take a cue from the physics of Newtonian gravity and assume that the filament interacts with

the other filaments in the same way its center of mass would interact with an imaginary, “center of mass” filament. We motivate this assumption from the Monte Carlo results on point vortices of Lim and Assad [2005] that showed a “flat-top”, cylindrical probability distribution for vortices in the plane. A nearly uniform, symmetric distribution is crucial to the center-of-mass assumption.

Given a point on filament i , $\psi_i(\tau)$, if the filament’s center-of-mass interacts with the center of mass of the other filaments, the interaction potential, V_i , simplifies:

$$\begin{aligned} \langle V_i(\tau) \rangle &= \left\langle \sum_j -\frac{1}{2} \log |\psi_i(\tau) - \psi_j(\tau)| \right\rangle \\ &\approx \langle -(N-1) \frac{1}{2} \log |\psi_i(\tau)| \rangle \approx \langle -N/4 \log |\psi_i(\tau)|^2 \rangle \\ &\approx \left\langle -N/4 \log \left(L^{-1} \int_0^L d\tau |\psi_i(\tau)|^2 \right) \right\rangle \\ &= \left\langle -N/4 \log \frac{I_N}{LN} \right\rangle, \end{aligned}$$

where we can say for large N that $N-1 \sim N$. This result makes the interaction a function of the angular momentum. This is to say that,

$$\langle |\psi_i(\tau) - \psi_j(\tau)|^2 \rangle \approx L^{-1} \left\langle \int_0^L d\tau |\psi_i(\tau)|^2 \right\rangle. \quad (4.6)$$

Because this mean-field assumption causes the filaments to be statistically independent, we no longer use the i subscript and call the position of the single, mean filament $\psi(\tau)$.

The center-of-mass assumption liberates us in the evaluation of the partition function, because we need to consider *neither* the configurations of other filaments *nor* their density distribution, whereas Lions and Majda do take the latter into account. All we need consider is the angular momentum.

4.3 Spherical Constraint

Given the mean-field, center-of-mass assumption, we have a new Hamiltonian system governing the behavior of N independent filaments is:

$$H'_N = N \left[\int_0^L d\tau \frac{\alpha}{2} \left| \frac{\partial \psi}{\partial \tau} \right|^2 - \frac{N}{4} \log \int_0^L d\tau |\psi(\tau)|^2 \right], \quad (4.7)$$

which, for M -linear-segment filaments, reads

$$H'_N(M) = N\alpha \sum_{k=1}^M \frac{1}{2} \frac{|\psi(k+1) - \psi(k)|^2}{\delta} - N^2/4 \sum_{k=1}^M \delta \log \frac{I_N(M)}{LN}, \quad (4.8)$$

where $H'_N(M)$ only differs from $H_N(M)$ (Equation 3.9) in the second term, and the new partition function reads

$$Z'_N(M) = \left\{ \int \frac{d\Psi}{a^M} \exp(-\beta H'_N(M) - \mu I_N(M)) \right\}^N, \quad (4.9)$$

where the Feynman scaling, $a = \pi L / (\alpha \beta M)$, (Feynman and Wheeler [1948]).

Returning to our derivation for the length scale, R , we take the simplest course possible to give a reasonable formula and impose a constraint on the filament,

$$L^{-1} \int_0^L d\tau |\Psi(\tau)|^2 = R^2 = \sum_{k=1}^M M^{-1} |\psi(k)|^2, \quad (4.10)$$

which imposes an average distance from the origin over the length of the filament. We include this constraint as a micro-canonical or exact constraint into the partition function,

$$Z''_N(M) = \left\{ \int \frac{d\Psi}{a^M} e^{(-\beta H'_N(M) - \mu I_N(M))} \delta(MR^2 - I_N(M)) \right\}^N. \quad (4.11)$$

This constraint eliminates fluctuations in interaction energy and angular momentum, leaving only fluctuations in local self-induction energy. This elimination provides the best opportunity for comparison with the 2D length scale work of Lim and Assad [2005] that also eliminates these two types of fluctuation.

Equation 4.11 is a multi-dimensional Gaussian integral with a spherical constraint—so called because it forces the vector Ψ to stay on the $M - 1$ -sphere of radius \sqrt{MR} . To evaluate it we turn to the spherical model of Berlin and Kac [1952].

The spherical model comprises a number of steps for evaluating integrals of the form of Equation 4.11, beginning by putting the Dirac-delta function into integral form and ending with a steepest descent evaluation of the integral over Ψ .

In integral (Fourier) form the Dirac-delta reads:

$$\delta \left(MR^2 - \sum_{k=1}^M |\psi(k)|^2 \right) = \int_{s_0-i\infty}^{s_0+i\infty} \frac{ds}{2\pi i} \exp \left[s \left(MR^2 - \sum_{k=1}^M |\psi(k)|^2 \right) \right], \quad (4.12)$$

and allows us to combine the function in the exponent in Equation 4.11 with the exponent of the spherical constraint. (Whereas before s was used as a symbol for microstate, here it is an integration variable.)

4.4 Free Energy Derivation for Radius

Now we can determine the free energy functional, which ought to be minimal under the constraints of the system, via steepest descent. Determining the free energy as a function of the particular statistic, R , is more useful than having an equation for the partition function itself because we can determine R by minimizing the free energy w.r.t. it and then solving for R .

Theorem 4.4.1. *Given the partition function defined in Equation 4.11 and the free energy in Equation 4.1, as $M \rightarrow \infty$, the value for R^2 giving minimal free energy is,*

$$R^2 = \frac{\beta^2 \alpha N + \sqrt{\beta^4 \alpha^2 N^2 + 32 \alpha \beta \mu}}{8 \alpha \beta \mu}. \quad (4.13)$$

Proof. The steepest descent method is an excellent way to obtain values for the minimum free energy. In employing steepest descent, we need to start with an integral of the form, $\int dx e^{-MF[x]}$. Then if $F[x_0] < F[x] \forall x \neq x_0$, i.e. its minimum value is at x_0 ,

$$\lim_{M \rightarrow \infty} M^{-1} \log \left(\int dx e^{-MF[x]} \right) = F[x_0].$$

This works because, as M increases, the distribution that $e^{-MF[x]}$ represents becomes narrower and focuses on x_0 until the distribution has zero value at all other x .

To take this approach, we put the partition function (dropping the double prime) in the appropriate form: If

$$Z_N(M) = \left\{ \int \frac{d\Psi}{a^M} \int_{s_0-i\infty}^{s_0+i\infty} \frac{ds}{2\pi i} e^{-MF[s]} \right\}^N, \quad (4.14)$$

then

$$F[s] = \alpha\beta M^{-1} \sum_{k=1}^M \frac{1}{2} \frac{|\psi(k+1) - \psi(k)|^2}{\delta} - N\beta LM^{-1}/4 \log R^2 \\ + \mu LM^{-1} R^2 - s \left(R^2 - \sum_{k=1}^M M^{-1} |\psi(k)|^2 \right), \quad (4.15)$$

is the non-dimensional free energy, where we have already applied the Dirac delta function to the interaction energy and the angular momentum.

We can pull the constant terms out of the integral over Ψ . Because F is positive definite, under Fubini's theorem we may switch the integrals to obtain

$$Z_N(M) = \left\{ e^{N\beta L/4 \log R^2 - \mu LR^2} \int_{s_0-i\infty}^{s_0+i\infty} \frac{ds}{2\pi i} \int \frac{d\Psi}{a^M} e^{-F'[s]} \right\}^N, \quad (4.16)$$

where

$$F'[s] = \alpha\beta \sum_{k=1}^M \frac{1}{2} \frac{|\psi(k+1) - \psi(k)|^2}{\delta} + s \left(\sum_{k=1}^M |\psi(k)|^2 - MR^2 \right), \quad (4.17)$$

is the free energy still dependent on Ψ .

The interior integral needs evaluation. Let

$$Z'(M) = \int_{s_0-i\infty}^{s_0+i\infty} \frac{ds}{2\pi} \int \frac{d\Psi}{A^M} e^{-F'[s]}, \quad (4.18)$$

be that interior. Let us put F' in matrix form:

$$F'[s] = -sMR^2 + K\Psi^\dagger A\Psi + s\Psi^\dagger \Psi, \quad (4.19)$$

where $K = \alpha\beta/\delta$, and the $M \times M$ matrix A has the form

$$\begin{aligned} A_{i,i} &= 1, \\ A_{i,i+1} &= A_{i+1,i} = A_{1,M} = A_{M,1} = -\frac{1}{2}, \\ A_{i,j} &= 0 \quad \text{other } i, j. \end{aligned}$$

The integral in Equation 4.18 is Gaussian. We can evaluate it, knowing the eigenvalues of the matrix A . These eigenvalues have the form $\lambda_i = 1 - \cos(2\pi(i-1)/M)$, (not related to the previous use of λ_i as strength of vorticity)(Berlin and Kac [1952], Lions and Majda [2000]) and so

$$Z'(M) = \int_{s_0-i\infty}^{s_0+i\infty} \frac{ds}{2\pi} e^{sMR^2} \left(\frac{\alpha\beta M}{L} \right)^M \prod_i \frac{1}{s + K\lambda_i}. \quad (4.20)$$

We need to put $Z'(M)$ back into the correct form for steepest descent. Following the example of Berlin and Kac, let $s = K(\eta - 1)$ then

$$\begin{aligned} Z'(M) &= \int_{\eta_0-i\infty}^{\eta_0+i\infty} \frac{d\eta}{2\pi} K \left(\frac{\alpha\beta M}{L} \right)^M (\eta - 1)^{-1} e^{-M \log(K)} e^{Mf[\eta]} \\ &= \int_{\eta_0-i\infty}^{\eta_0+i\infty} \frac{d\eta}{2\pi} K (\eta - 1)^{-1} e^{Mf[\eta]}, \end{aligned} \quad (4.21)$$

where

$$f[\eta] = KR^2(\eta - 1) - M^{-1} \sum_{i=2}^M \log(\eta - \cos(2\pi(i-1)/M)), \quad (4.22)$$

and $\eta \geq 1$.

We leave the $i = 1$ term out of the sum in $f[\eta]$ so that we can evaluate f further by taking the limit on the second term,

$$\lim_{M \rightarrow \infty} M^{-1} \sum_{i=2}^M \log(\eta - \cos(2\pi(i-1)/M)) = \frac{1}{2\pi} \int_0^{2\pi} d\omega \log(\eta - \cos(\omega)),$$

which gives

$$\begin{aligned} f[\eta] &= KR^2(\eta - 1) - \frac{1}{2\pi} \int_0^{2\pi} d\omega \log(\eta - \cos(\omega)) \\ &= KR^2(\eta - 1) - \log(\eta + (\eta^2 - 1)^{\frac{1}{2}}). \end{aligned} \quad (4.23)$$

To apply steepest descent, we determine the saddle point $\eta = \eta_0$ where $f[\eta]$ has its minimum value, $f[\eta_0]$. Taking the derivative and setting it equal to zero,

$$\frac{\partial f}{\partial \eta} = KR^2 - \frac{1}{\sqrt{\eta^2 - 1}} = 0, \quad (4.24)$$

implies

$$\eta_0 = \sqrt{\frac{1}{(KR^2)^2} + 1}. \quad (4.25)$$

Having evaluated f , we can give an equation for the original free energy,

$$F[\eta_0] = -N\beta L/4 \log R^2 + \mu LR^2 - Mf[\eta_0], \quad (4.26)$$

and evaluate it as $M \rightarrow \infty$.

Now we fill in the expression for η_0 as defined above:

$$\begin{aligned} \lim_{M \rightarrow \infty} Mf[\eta_0] &= \lim_{M \rightarrow \infty} KR^2(\eta_0 - 1) - M \log(\eta_0 + (\eta_0^2 - 1)^{\frac{1}{2}}) \\ &= \lim_{M \rightarrow \infty} MKR^2 \left(\sqrt{\frac{1}{(KR^2)^2} + 1} - 1 \right) - M \log \left(\sqrt{\frac{1}{(KR^2)^2} + 1} + \frac{1}{KR^2} \right) \end{aligned} \quad (4.27)$$

which, because it is an energy for a filament, ought to be finite. The first term is the energy of the filament, E_{fil} , and the second, the entropy, S_{fil} , and each by itself is finite, so we take each limit separately.

The energy limit is simple to calculate using L'Hôpital's rule:

$$\begin{aligned}
E_{fil} &= \lim_{M \rightarrow \infty} M \frac{\alpha\beta M}{L} R^2 \left(\sqrt{\frac{L^2}{(\alpha\beta M R^2)^2} + 1} - 1 \right) \\
&= \lim_{\delta \rightarrow 0} L \frac{\alpha\beta}{\delta^2} R^2 \left(\sqrt{\frac{\delta^2}{(\alpha\beta R^2)^2} + 1} - 1 \right) \\
&= \lim_{\delta \rightarrow 0} L \frac{\alpha\beta}{2\delta} R^2 \left(\left(\frac{\delta^2}{(\alpha\beta R^2)^2} + 1 \right)^{-\frac{1}{2}} \frac{\delta}{(\alpha\beta R^2)^2} \right) \\
&= \frac{L}{2\alpha\beta R^2}
\end{aligned} \tag{4.28}$$

The entropy limit is equally simple:

$$\begin{aligned}
S_{fil} &= \lim_{M \rightarrow \infty} M \log \left(\sqrt{\frac{1}{(\frac{\alpha\beta M}{L} R^2)^2} + 1} + \frac{1}{\frac{\alpha\beta M}{L} R^2} \right) \\
&= \lim_{\delta \rightarrow 0} \frac{L}{\delta} \log \left(\sqrt{\frac{\delta^2}{(\alpha\beta R^2)^2} + 1} + \frac{\delta}{\alpha\beta R^2} \right) \\
&= \lim_{\delta \rightarrow 0} L \left[\sqrt{\frac{\delta^2}{(\alpha\beta R^2)^2} + 1} + \frac{\delta}{\alpha\beta R^2} \right]^{-1} \left[\left(\frac{\delta}{(\alpha\beta R^2)^2} + 1 \right)^{-\frac{1}{2}} \frac{\delta}{(\alpha\beta R^2)^2} + \frac{1}{\alpha\beta R^2} \right] \\
&= \frac{L}{\alpha\beta R^2}
\end{aligned} \tag{4.29}$$

These two results imply that

$$\lim_{M \rightarrow \infty} M f[\eta_0] = -\frac{L}{2\alpha\beta R^2}$$

and

$$F[\eta_0] = L\mu R^2 - N\beta L/4 \log R^2 + \frac{L}{2\alpha\beta R^2}. \tag{4.30}$$

We minimize with respect to R^2 ,

$$\frac{\partial F}{\partial R^2} = L\mu - \frac{N\beta L}{4R^2} - \frac{L}{2\alpha\beta R^4} = 0, \tag{4.31}$$

and solve for R^2 ,

$$\begin{aligned} R^2 &= \frac{N\beta/4 \pm \sqrt{(N\beta/4)^2 + 4\mu\frac{1}{2\alpha\beta}}}{2\mu} \\ &= \frac{\beta^2\alpha N + \sqrt{\beta^4\alpha^2 N^2 + 32\alpha\beta\mu}}{8\alpha\beta\mu}, \end{aligned} \quad (4.32)$$

where we take the “plus” solution as giving physical results. \square

We note that the relationship between $F[\eta_0]$ and our previous F_N in Equation 4.1 is $F[\eta_0] = \beta F_N$, meaning that $F[\eta_0]$ is non-dimensional while F_N has units of energy.

The resulting expression for the square length scale R^2 is useful for comparison with the length scale result of Lim and Assad [2005] because, if we take the limit

$$\lim_{\alpha \rightarrow \infty} \frac{\beta^2\alpha N + \sqrt{\beta^4\alpha^2 N^2 + 32\alpha\beta\mu}}{8\alpha\beta\mu} = \frac{N\beta}{4\mu}, \quad (4.33)$$

we get back the 2D point vortex result for the length scale, which shows that our formula and the Lim and Assad [2005] formula agree for perfectly straight filaments.

However, for finite α the two formulas show a significant difference. The 2D formula is linear in β , our formula is non-linear. In fact, for decreasing β , the sign of the slope of our formula changes at $\beta = \beta_0$, where

$$\beta_0^3 = \frac{4\mu}{\alpha N^2}. \quad (4.34)$$

That the system collapses and then starts to expand as “temperature”, $1/\beta$, increases indicates a significant departure from the strictly-2D where the system size only collapses. In Chapter 5.2, we show that that Monte Carlo confirms this result and that the straightness assumptions of the model hold through much of the expansion phase.

CHAPTER 5

Monte Carlo

5.1 Algorithm

Path Integral Monte Carlo methods emerged from the path integral formulation invented by Dirac that Richard Feynman later expanded (Zee [2003]), in which particles are conceived to follow all paths through space. One of Feynman’s great contributions to the quantum many-body problem was the mapping of path integrals onto a classical system of interacting “polymers” (Feynman and Wheeler [1948]). D. M. Ceperley used Feynman’s convenient piecewise linear formulation to develop his PIMC method which he successfully applied to He-4, generating the well-known lambda transition for the first time in a microscopic particle simulation (Ceperley [1995]). Because it describes a system of interacting polymers, PIMC applies to classical systems that have a “polymer”-type description like nearly parallel vortex filaments.

PIMC has several advantages. It is a *continuum* Monte Carlo algorithm, relying on no spatial lattice. Only time (length in the z-direction in the case of vortex filaments) is discretized, and the algorithm makes no assumptions about types of phase transitions or trial wavefunctions.

The Monte Carlo simulation begins with a random distribution of filament end-points in a square of side 10, and there are two possible moves that the algorithm chooses at random:

1. Moves a filament’s end-points, $\psi_i(1)$ and $\psi_i(M + 1)$. The index i is chosen at random, and the filament i ’s end-points moved a uniform random distance.
2. Keeps end-points stationary and, following the bisection method of Ceperley (Figure 5.1), grows a new internal configuration for a randomly chosen filament (Ceperley [1995]).

In each case, the energy of the new state, s' , is calculated and retained with

probability

$$A(s \rightarrow s') = \min \left\{ 1, \exp \left(-\beta [H_N^{s'}(M) - H_N^s(M)] - \mu [I_N^{s'}(M) - I_N^s(M)] \right) \right\}, \quad (5.1)$$

where s is the previous state. This effectively samples states from the Gibbs probability distribution in Equation 3.10.

Our stopping criteria is graphical in that we ensure that the cumulative arithmetic mean of the energy,

$$E_{cum}^k = k^{-1} \sum_{i=1}^k H_N(s_i) + \frac{\mu}{\beta} I_N(s_i), \quad (5.2)$$

where s_i refers to the state resulting from the i th move and k is the current move index, settles to a constant. The energy is almost guaranteed to settle in the case of the Gibbs' measure because of the tendency for the system to select a particular energystate (mean energy) and remain close to that state. Typically, we run for 1 million moves (accepted plus rejected) or 50,000 sweeps for 20 vortices. Afterwards, we collect data from about 200,000 moves (1000 sweeps) to generate statistical information.

5.2 Simulation Results

5.2.1 Comparison

We simulated a collection of $N = 20$ vortices each with a piecewise linear representation with $M = 1024$ segments and ran the system to equilibration, determined by the settling of the mean and variance of the total energy. We ran the system for 20 logarithmically spaced values of β between 0.001 and 1 plus two points, 10 and 100. We set $\alpha = 10^7$ (enforcing straightness), $\mu = 2000$, and $L = 10$. Decreasing β simulates an increase in temperature, $1/\beta$. We calculate two arithmetic averages: the mean square vortex position,

$$R_{MC}^2 = (MN)^{-1} \sum_{i=1}^N \sum_{k=1}^M |\psi_i(k)|^2, \quad (5.3)$$

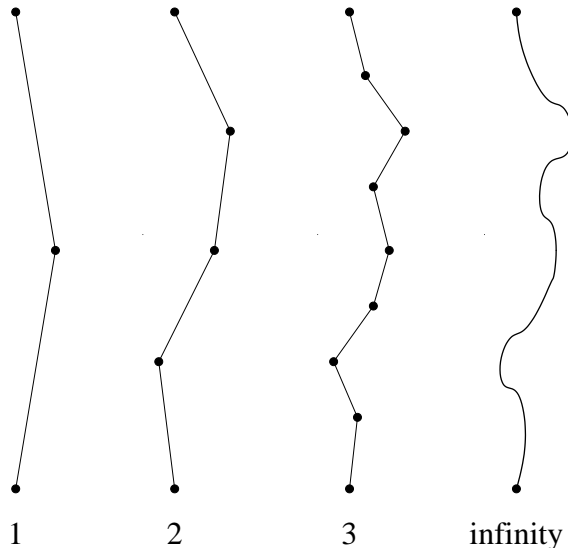


Figure 5.1: The bisection algorithm works by bisecting the filament to sample point positions. First the center point is selected, then the two points half-way from the center to the end-points, then four more points, eight, and so on until some maximum number of points are sampled. These are snapshots of one filament at different steps in the sampling process.

and the mean square amplitude per segment,

$$a^2 = (MN)^{-1} \sum_{i=1}^N \sum_{k=1}^M |\psi_i(k) - \psi_i(k+1)|^2, \quad (5.4)$$

where $\psi_i(M+1) = \psi_i(1)$.

Measures of the Monte Carlo R_{MC}^2 , Equation 5.3, correspond well to the 3D R^2 , Equation 4.32, in Figure 5.2 whereas, the strictly-2D R_{2D}^2 , Equation 2.10, continues to decline when the others curve up with decreasing β values, suggesting that the 3-D effects are not only real in the Monte Carlo but that the mean-field is a good approximation with these parameters. In Section 7.1 we discuss what this expansion really means.

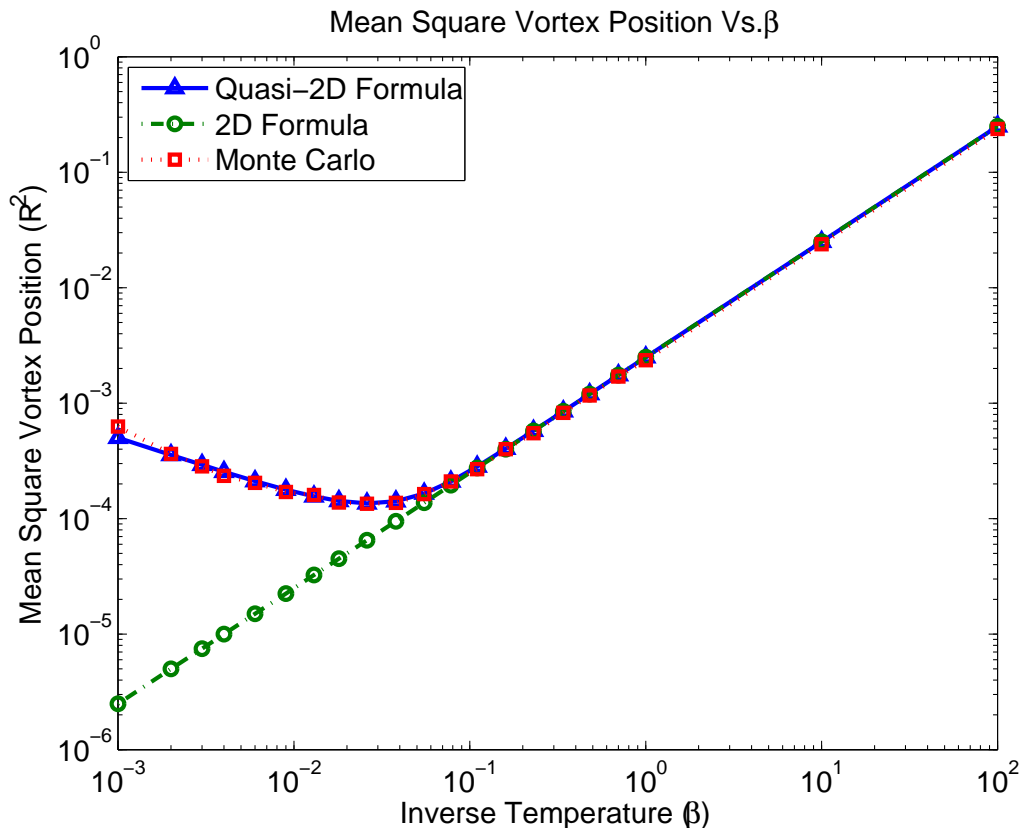


Figure 5.2: The mean square vortex position, defined in Equation 5.3, compared with Equations 4.32 and 2.10 shows how 3-D effects come into play around $\beta = 0.16$. That the 2D formula continues to decrease while the Monte Carlo and the quasi-2D formula curve upwards with decreasing β suggests that the internal variations of the vortex lines have a significant effect on the probability distribution of vortices.

5.2.2 Straightness Holds

In order to be considered straight enough, we need

$$a \ll \frac{L}{M} = \frac{10}{1024} \sim 0.0098. \quad (5.5)$$

Straightness holds for all β values, shown in Figure 5.3. These conditions hold on average. We ignore extreme low-probability cases as not contributing significantly to the statistics. These straightness constraints, coupled with filaments having no attractive interactions, mean hairpins (kinks or, in quantum terminology, instantons)

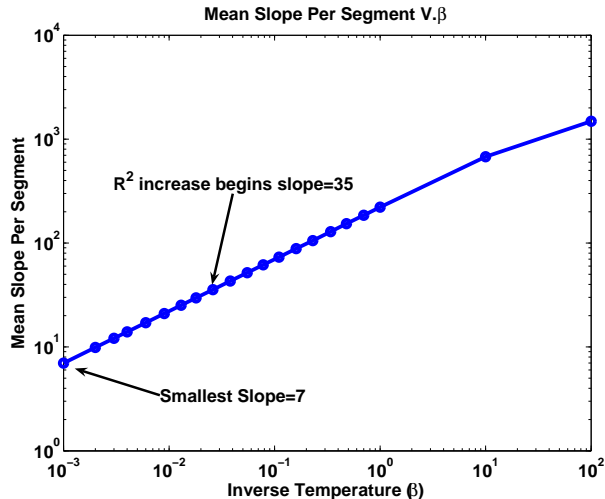


Figure 5.3: This figure shows the mean slope per segment, δ/a , where $\delta \sim 0.0098$ and a is given by Equation 5.4, and that straightness holds for all β values. The point at which R^2 begins to increase with decreasing β (Figure 5.2) has a mean slope of 35, and, even at the smallest $\beta = 10^{-3}$, the segments have an average angle of 82° with respect to the complex plane.

do not occur.

Aside from straightness constraints, the reader might question whether allowing vortex filaments to entangle violates the model's assumptions. While this is a valid concern, it is not an assumption of the model. Since this fluid is almost-everywhere inviscid, it contains asymptotically small regions of non-zero viscosity, and, while a totally inviscid fluid cannot allow vortices to change topology (cross over each other) from state to state, an almost-everywhere inviscid fluid allows vortex reconnections and cross-overs to occur due to microscopic viscous effects. Therefore, in our simulations vortices are allowed to cross one-another. We are not claiming to model vortex reconnection, which is a mysterious process, but only the before and after effects of it.

Concerning the question of how vortices can cross one-another and still remain nearly parallel, we point to the extremely high-density (tiny value of R^2) which allows even the straightest filaments to entangle.

CHAPTER 6

Microcanonical Ensembles

The success of our mean-field approximation for the canonical system leads us to consider a statistical ensemble for which there is no existing Monte Carlo algorithm—the microcanonical. Requiring energy and angular momentum to be fixed, the PIMC algorithm is no longer applicable in its current form. Therefore, we proceed analytically to a closed form solution for specific heat. For this Chapter we take $L = 1$ without loss of generality.

Since magnetically confined plasmas should be isolated with conserved angular momentum, the correct model is microcanonical in enthalpy and angular momentum:

$$P_{\text{MCE}}(s) = Z_{\text{MCE}}^{-1} \delta(NH_0 - H_N - pM_N) \delta(NR^2 - M_N), \quad (6.1)$$

where H_0 is the total enthalpy per vortex per period of the plasma and $Z_{\text{MCE}} = \int ds \delta(NH_0 - H_N - pM_N) \delta(NR^2 - M_N)$. Here H_N is the mean-field Hamiltonian. It is our intent to allow R^2 to be determined by other parameters in the system and keep enthalpy and pressure, p , fixed.

We now proceed to derive an explicit formula for the maximal entropy of this system in the non-extensive thermodynamic limit. We refer the reader to Horwitz [1983] for the following procedure: Given our previous assumptions about the enthalpy, the entropy per filament, S , is defined by,

$$e^{NS} = \int D\psi \delta(NH_0 - H_N - pNR^2) \delta(NR^2 - M_N). \quad (6.2)$$

This definition implies,

$$S = \frac{1}{N} \log \left[\int D\psi \delta(NH_0 - H_N - pNR^2) \delta(NR^2 - M_N) \right]. \quad (6.3)$$

We need to find R^2 as a minimization of the canonical free enthalpy as we did in Chapter 4. Replacing the first delta function with its integral representation

yields,

$$e^{NS} = \int D\psi \int_{\beta_0 - i\infty}^{\beta_0 + i\infty} \frac{d\beta}{2\pi i} e^{\beta NH_0 - \beta H_N - \beta NR^2} \delta(NR^2 - M_N). \quad (6.4)$$

In the broken-segment model this is,

$$e^{NS} = \lim_{M \rightarrow \infty} e^{NS_N(M)} \quad (6.5)$$

where

$$e^{NS(M)} = \int \frac{d\Psi}{a^M} \int_{\beta_0 - i\infty}^{\beta_0 + i\infty} \frac{d\beta}{2\pi i} e^{\beta NH_0 - \beta H_N(M)} \delta(NMR^2 - N\Psi^\dagger \Psi), \quad (6.6)$$

and $a = \pi/(\alpha\beta_0 M)$.

Given the obviously finite result above, we can rewrite the entropy relation as,

$$\begin{aligned} e^{NS(M)} &= \int \frac{d\beta}{2\pi i} e^{\beta NH_0} \int \frac{d\Psi}{a^M} \exp(-\beta H_N(M)) \delta(MR^2 - \Psi^\dagger \Psi) \\ &= \int \frac{d\beta}{2\pi i} e^{\beta NH_0} [Z_{can}(M)]^N \end{aligned} \quad (6.7)$$

where

$$Z_{can}(M) = \int \frac{d\Psi}{a^M} \exp(-K\Psi^\dagger A\Psi - \beta pR^2 + \beta N/4 \log R^2) \delta(MR^2 - \Psi^\dagger \Psi) \quad (6.8)$$

is the partition function for the non-thermally-isolated system of Chapter 4.

Now we need to take the steepest-descent limit to find the maximal entropy,

$$S_{max}(H_0) = \lim_{N \rightarrow \infty} \lim_{M \rightarrow \infty} S(M). \quad (6.9)$$

Because our mean-field approximation is a subset of theirs, Lions and Majda [2000] have proven the existence of these thermodynamic limits.

Writing out the full expression:

$$e^{NS_N} = \lim_{M \rightarrow \infty} e^{NS_N(M)} = \lim_{M \rightarrow \infty} \int \frac{d\beta}{2\pi i} e^{\beta NH_0} [Z_{can}(M)]^N. \quad (6.10)$$

We have already found an approximation for the free energy as $F = -\lim_{M \rightarrow \infty} \frac{1}{\beta} \log Z_{can}(M)$. We know that if we make the scaling $\beta' = \beta N$, $\alpha' = \alpha/N$, $p' = p/N$, and $H'_0 = H_0/N$ in anticipation of taking the $N \rightarrow \infty$ limit, we have the free energy as,

$$F = p'R^2 - 1/4 \log R^2 + \frac{1}{2\alpha'\beta'^2 R^2}, \quad (6.11)$$

where

$$R^2 = \frac{\beta'^2 \alpha' + \sqrt{\beta'^4 \alpha'^2 + 32\alpha'\beta'^2 p'}}{8\alpha'\beta'^2 p'}, \quad (6.12)$$

minimizes F .

Because the limit as $M \rightarrow \infty$ of the integral over β is finite (a well-known result in quantum field theory (Lawson [2000])), we can bring the limit inside. Replacing $\lim_{M \rightarrow \infty} [Z_{can}(M)]^N$ with $\exp(-\beta' NF)$, gives

$$e^{NS_N} = \int \frac{d\beta'}{2\pi i} e^{\beta' NH'_0 - \beta' NF}, \quad (6.13)$$

and, because $S_{max} = \lim_{N \rightarrow \infty} S_N$,

$$\begin{aligned} S_{max}(H_0) &= \beta'_0 H'_0 - \beta'_0 F \\ &= \beta'_0 H'_0 + \frac{\beta'_0}{4} \log(R^2) - \frac{1}{2\alpha\beta_0 R^2} - \beta'_0 p' R^2. \end{aligned} \quad (6.14)$$

This entropy is exact within the mean-field assumption for $N \rightarrow \infty$.

We find the unknown multiplier, β_0 , by relating the enthalpy per filament parameter, H_0 , to the mean enthalpy, $NH_0 = \langle H_N + pM_N \rangle$, where $\langle \cdot \rangle$ denotes average against Equation 6.1.

By definition the average enthalpy is given by

$$\langle H_N + pM_N \rangle = \frac{\int D\psi H_N \delta(NH_0 - H_N - pM_N) \delta(NR^2 - M_N)}{\int D\psi \delta(NH_0 - H_N - pM_N) \delta(NR^2 - M_N)}. \quad (6.15)$$

We can simplify this equation with steepest-descent methods in the non-extensive

limit, following Horwitz [1983]:

$$\begin{aligned}
e^{NS_N} &= \int D\psi \delta(NH_0 - H_N - pM_N) \delta(NR^2 - M_N) \\
&= \int D\psi \int_{\beta_0 - i\infty}^{\beta_0 + i\infty} \frac{d\beta}{2\pi i} e^{\beta NH_0} e^{-\beta H_N - \beta p M_N} \delta(NR^2 - M_N) \quad (6.16)
\end{aligned}$$

Therefore, we can give the average enthalpy in integral form using a derivative,

$$\langle H_N + pM_N \rangle = \frac{\int D\psi \int_{\beta_0 - i\infty}^{\beta_0 + i\infty} \frac{d\beta}{2\pi i} e^{\beta NH_0} \left(-\frac{\partial}{\partial \beta} e^{-\beta(H_N + pNR^2)} \right) \delta(NR^2 - M_N)}{\int D\psi \int_{\beta_0 - i\infty}^{\beta_0 + i\infty} \frac{d\beta}{2\pi i} e^{\beta NH_0} e^{-\beta(H_N + pNR^2)} \delta(NR^2 - M_N)}. \quad (6.17)$$

In the non-extensive, asymptotic limit, this simplifies to

$$\langle H_N + pM_N \rangle \approx N \frac{\int_{\beta'_0 - i\infty}^{\beta'_0 + i\infty} \frac{d\beta'}{2\pi i} e^{\beta' NH'_0} \left(-\frac{\partial}{\partial \beta'} e^{-\beta' NF} \right)}{\int_{\beta'_0 - i\infty}^{\beta'_0 + i\infty} \frac{d\beta'}{2\pi i} e^{\beta' NH'_0} e^{-\beta' NF}}. \quad (6.18)$$

We have replaced $\int D\psi e^{-\beta H_N - \beta p R^2}$ with $\exp(-\beta' NF)$ from above. This replacement requires an interchange of the integral and the derivative. We offer a proof that this replacement is valid:

Lemma 6.0.1. *The following equation is true:*

$$\begin{aligned}
&\lim_{M \rightarrow \infty} \int d\Psi / a^M \frac{\partial}{\partial \beta} e^{-\beta(H_N(M) + pNR^2)} \delta(NR^2 - M_N(M)) \\
&= \frac{\partial}{\partial \beta} \exp(-\beta NF). \quad (6.19)
\end{aligned}$$

Proof. There are two separate issues here:

1. whether the derivative can be brought out of the integral:

$$\begin{aligned}
&\int d\Psi / a^M \frac{\partial}{\partial \beta} e^{-\beta(H_N(M) + pNR^2)} \delta(NR^2 - M_N(M)) \\
&= \frac{\partial}{\partial \beta} \int d\Psi / a^M e^{-\beta(H_N(M) + pNR^2)} \delta(NR^2 - M_N(M)), \quad (6.20)
\end{aligned}$$

2. whether the derivative can be brought out of the limit:

$$\begin{aligned} & \lim_{M \rightarrow \infty} \frac{\partial}{\partial \beta} \int d\Psi/a^M e^{-\beta(H_N(M)+pNR^2)} \delta(NR^2 - M_N(M)) \\ &= \frac{\partial}{\partial \beta} \lim_{M \rightarrow \infty} \int d\Psi/a^M e^{-\beta(H_N(M)+pNR^2)} \delta(NR^2 - M_N(M)). \end{aligned} \quad (6.21)$$

Equation 6.20 is true if and only if

$$\int d\Psi/a^M e^{-\beta(H_N(M)+pNR^2)} \delta(NR^2 - M_N(M)) < \infty, \quad (6.22)$$

and the integrand is differentiable. The equation is integrable because the integrand is positive definite (and positive). Therefore, it is a simple Gaussian integral. The smoothness of the integrand guarantees differentiability.

For 6.21, we prove it explicitly, i.e. calculate the derivative first and then take the limit. If M is large, we can make the approximation:

$$\int d\Psi/a^M e^{-\beta(H_N(M)+pNR^2)} \delta(NR^2 - M_N(M)) \approx e^{-\beta NF(M)}, \quad (6.23)$$

where

$$F(M) = pR^2 - N/4 \log R^2 - \frac{M^2 \alpha}{\beta} R^2 (\eta_0 - 1) - \frac{M}{\beta} \log(\eta_0 + (\eta_0^2 - 1)^{\frac{1}{2}}) \quad (6.24)$$

and

$$\eta_0 = \sqrt{\frac{1}{(M\alpha\beta R^2)^2} + 1}. \quad (6.25)$$

Taking the derivative,

$$-\frac{\partial}{\partial \beta} e^{-\beta NF(M)} = NF(M) e^{-\beta NF(M)} F_\beta(M), \quad (6.26)$$

it is trivial to show that

$$\lim_{M \rightarrow \infty} NF(M) e^{-\beta NF(M)} F_\beta(M) = NF e^{-\beta NF} F_\beta = -\frac{\partial}{\partial \beta} e^{-\beta NF}. \quad (6.27)$$

□

As N becomes large, the saddle point method gives

$$\langle H_N + pM_N \rangle \approx N \frac{e^{\beta'_0 N H'_0} \left(-\frac{\partial}{\partial \beta'_0} e^{-\beta'_0 N F} \right)}{e^{\beta'_0 N H'_0} e^{-\beta'_0 N F}}, \quad (6.28)$$

which implies that, because $N^2 H'_0 = \langle H_N \rangle$,

$$\begin{aligned} H'_0 &= \lim_{N \rightarrow \infty} -\frac{1}{N} \frac{\partial e^{-\beta'_0 N F}}{\partial \beta'_0} \frac{1}{e^{-\beta'_0 N F}} = \lim_{N \rightarrow \infty} -\frac{1}{N} \frac{\partial \log e^{-\beta'_0 N F}}{\partial \beta'_0}, \\ &= \frac{\partial}{\partial \beta'_0} \left(-\frac{\beta'_0}{4} \log R^2 + \frac{1}{2\alpha' \beta'_0 R^2} + \beta'_0 p' R^2 \right) \end{aligned} \quad (6.29)$$

exactly.

The above derivation confirms that we can find the average enthalpy in the thermodynamic limit using the canonical formulation, noting that R^2 is defined by Equation 6.12. The constants p , α , and β_0 are required to be positive for the model to have a finite partition function. We cannot give an explicit expression for β_0 because it is a root of a transcendental equation, but such is unnecessary for the following negative specific heat result:

We define specific heat at constant generalized pressure, p ,

$$c_p = -\beta_0^2 \frac{\partial H_0}{\partial \beta_0} = -\beta_0^2 \frac{\partial^2 \beta_0 F}{\partial \beta_0^2} \quad (6.30)$$

and after evaluating with Equation 6.29 and simplifying (dropping primes and 0-subscripts)

$$c_p = \frac{\beta}{4} \left(\frac{\alpha \beta^2}{\sqrt{\alpha \beta^2 (\alpha \beta^2 + 32p)}} - 1 \right). \quad (6.31)$$

Equation 6.31 is significant. It indicates that the specific heat is not only negative for this system, but *strictly* negative if parameters are non-zero (Figure 6.1). In the low-temperature (large β) case, for constant field strength, R^2 does not change significantly with temperature indicating that filaments are in a stable configuration for a large range of low-temperatures. Because the filaments do not move relative to one another at low-temperatures and the self-induction is negligible,

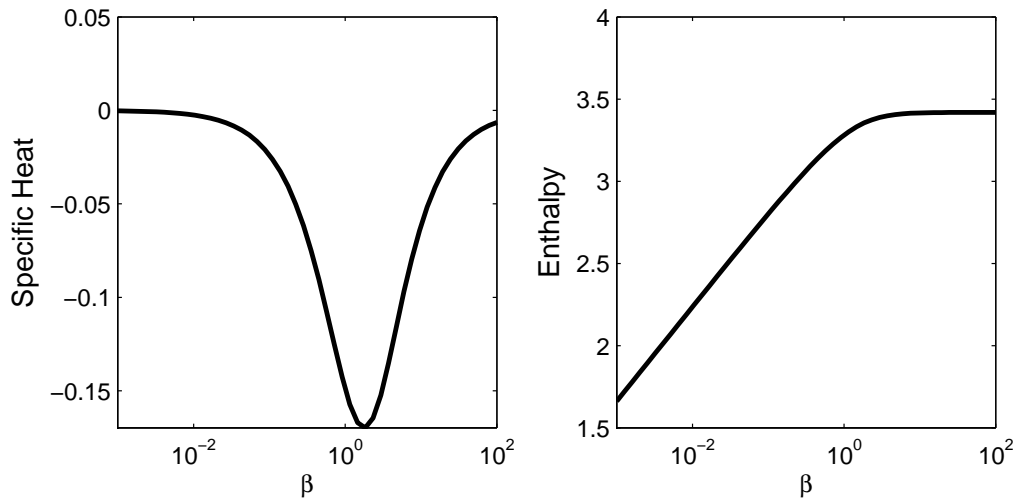


Figure 6.1: The specific heat at constant pressure (Equation 6.31) for the thermally isolated system is negative, meaning that the constant pressure Enthalpy Per Length (Equation 6.29) decreases with increasing temperature. (Here $\alpha' = 5 \times 10^5$ and $p' = 8 \times 10^4$.)

the enthalpy does not change. When temperature becomes high the internal entropy causes a massive expansion in the overall size of the system (Figure 6.2), and energy of the logarithmic interaction decreases far more than the enthalpy of the self-induction increases. The strong magnetic field absorbs this energy, but, since it is assumed to be an infinitely massive reservoir able to maintain the enthalpy at H_0 , the confinement remains constant.

On a side note, because the specific heat in Equation 6.31 does not cross the axis (i.e. is never positive) for any positive parameters, the expansion in R^2 in the canonical system is not likely a phase transition in β , but a continuous “transition” (Lynden-Bell and Lynden-Bell [1977]). The system appears to change behavior significantly, but it changes without any discontinuity in the free energy or specific heat.

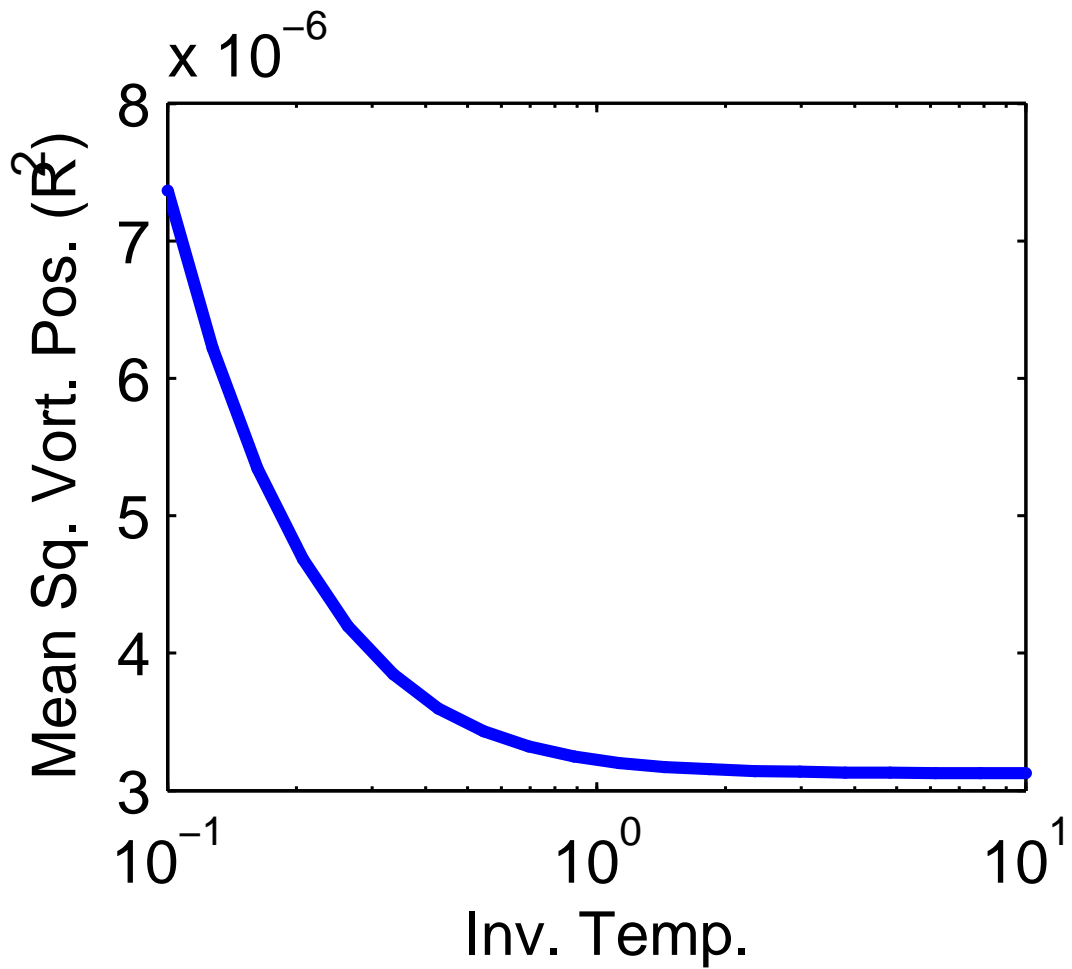


Figure 6.2: The Mean Square Vortex Position (Equation 6.12) increases exponentially at high temperature, while it is nearly constant at low-temperature. (Here $\alpha = 5 \times 10^5$ and $p = 8 \times 10^4$.)

CHAPTER 7

Discussion and Conclusions

7.1 Discussion

We have shown in the canonical ensemble that with increasing β there is a “transition” from decreasing R^2 , the 2D behavior, to increasing R^2 , the 3D behavior. We put this word “transition” in quotes because at present we have no proof for or against this being a phase transition. The free energy function that we derive is smooth for all positive β . However, this is not proof against there being a phase transition in the original system. At this point it is a subject for future research.

The decreasing- β , R -expansion suggests that, by adding degrees of freedom to the 2D model to make it a quasi-2D model, we add a mechanism for the vortices to resist confinement through entropic effects. As β decreases past the “transition”, the system’s R^2 goes from being the result of interaction-versus-angular momentum competition to an entropy-versus-angular momentum competition. In the 2D system this 3rd dimension entropy is not there. Although there is another kind of entropy in the 2D model that will slow the compression as $\beta \rightarrow 0$ to a constant value, it is not enough to cause an increase in the system size. In the 3D system, the degrees of freedom are exponentially greater, which causes the expansion seen in Figure 5.2.

As mentioned above the negative specific heat indicates a runaway reaction in the thermally microcanonical system that models strongly confined, single-sign generalized vortex filaments. We hypothesize that this kind of runaway reaction, observed in gravo-thermal collapse of globular clusters (Lynden-Bell and Wood [1968]), can lead to two possible outcomes: (1) a collapse similar to globular clusters in which an outer halo of columns separates from an inner core that collapses in on itself, possibly resulting in nuclear fusion, (2) a turbulent expansion of the entire system. Further research will focus on answering this question, but clearly 3D effects are crucial.

7.2 Conclusion

Statistical mechanics provides a way to model transitions in decaying turbulence when there is a separation of time scales. We conclude from our results that the transfer of the model size from an interaction-angular momentum competition to an entropy-angular momentum competition is a kind of transition to turbulence purely due to 3D effects. Whether it is a phase transition is unknown, but it shows that 3D effects do become significant in determining the length scale of the turbulent system, a useful result for experiments in tight confinement of rotating nearly-inviscid fluids.

The key role of angular momentum in the derivation of the expression for R^2 and the subsequent Monte Carlo validation cannot be over-emphasized. At positive β and α , quasi-2D vortices of the same sign effectively repulse one-another. Therefore, in the unbounded plane, they would fly off to infinity without the angular momentum constraint unless hemmed in by an infinite expanse of vortices, the case of periodic boundaries, or walls. As we mentioned in the introduction, walls and periodic boundaries enforce an artificial length scale on the vortices, while angular momentum constraints allow that length scale to be found naturally.

In experiments and simulations of experiments, it is often reasonable to model walls present in the experimental setup. However, in oceans and atmospheres and in stars, there are no walls, and, at scales where Coriolis effects are small, it does not make sense to use a spherical domain unless the simulation is of extremely high resolution. The proper regime for applications of unbounded plane, conserved angular momentum simulations is in small Rossby number regions where small-scale rotation occurs such as Julien et al. [1996] have modeled in their astrophysical simulations and found arrays of like-sign nearly parallel vortex filaments. To this niche we have contributed a previously unseen entropic transfer to turbulence in rotating, almost-everywhere ideal fluids.

In the EMH model, we have shown that the microcanonical and canonical ensembles are not equivalent by showing negative specific heat. We have also shown that, in the likely event of runaway collapse, if and only if energy, angular momentum, and particle volume can be kept fixed could a fusion reaction such as occurs deep within the stars begin.

BIBLIOGRAPHY

- A. A. Abrikosov. On the magnetic properties of superconductors of the second group. *Soviet Physics JETP*, 5(6):1442–52, 1957.
- T. D. Andersen and C. C. Lim. Explicit formulae for nearly parallel vortex filaments. Submitted to GAFD, Jan. 2007a.
- T. D. Andersen and C. C. Lim. Statistical equilibrium of trapped slender vortex filaments. Submitted to JFM, Feb. 2007b.
- T. D. Andersen and C. C. Lim. Negative specific heat in generalized quasi-2d vorticity. Submitted to Phys. Rev. Lett., Apr. 2007c.
- T. D. Andersen and C. C. Lim. Negative specific heat in magnetohydrodynamical plasmas. In Progress, Apr. 2007d.
- V. Berdichevsky. Statistical mechanics of vortex lines. *Phys. Rev. E*, 57:2885, 1998.
- V. Berdichevsky. On statistical mechanics of vortex lines. *Int. J. Eng. Sci.*, 40: 123–129, 2002.
- T. H. Berlin and M. Kac. The spherical model of a ferromagnet. *Phys. Rev.*, 86(6): 821, 1952.
- N. Bohr. PhD thesis, U. Copenhagen, 1911.
- Lowell S. Brown. *Quantum Field Theory*. Cambridge UP, Cambridge, 1992.
- A. J. Callegari and L. Ting. Motion of a curved vortex filament with decaying vortical core and axial velocity. *SIAM J. on Applied Math*, 35(1):148–175, 1978.
- D. M. Ceperley. Path integrals in the theory of condensed helium. *Rev. o. Mod. Phys.*, 67:279, April 1995.
- A. J. Chorin. *Vorticity and Turbulence*. Springer-Verlag, New York, 1994.

- M. T. DiBattista and A. Majda. Equilibrium statistical predictions for baroclinic vortices: The role of angular momentum. *Th. and Comp. Fluid Dyn.*, 14:293, 2001.
- S. F. Edwards and J. B. Taylor. Negative temperature states for a two-dimensional plasmas and vortex fluids. *Proc. R. Soc. Lond. A.*, 336:257–271, 1974.
- R. P. Feynman and J. W. Wheeler. Space-time approach to non-relativistic quantum mechanics. *Rev. o. Mod. Phys.*, 20:367, 1948.
- K. S. Fine, A. C. Cass, W. G. Flynn, and C. F. Driscoll. Relaxation of 2d turbulence to vortex crystals. *Phys. Rev. Lett.*, 75:3277–3280, 1973.
- A. V. Gordeev, A. S. Kingsep, and L. I. Rudakov. Electron magnetohydrodynamics. *Physics Reports*, 243:215, 1994.
- H. Hasimoto. A soliton on a vortex filament. *J. Fluid Mech.*, 51:472, 1972.
- G. Hornig. *Tubes, Sheets and Singularities in Fluid Dynamics*, volume 71 of *Fluid Mechanics and its Applications*. Kluwer, Boston, 2003.
- G. Horwitz. Steepest descent path for the microcanonical ensemble- resolution of an ambiguity. *Comm. Math. Phys.*, 89:117–129, 1983.
- G. R. Joyce and D. Montgomery. Negative temperature states for a two-dimensional guiding center plasma. *J. Plasma Phys.*, 10:107, 1973.
- K. Julien, S. Legg, J. McWilliams, and J. Werne. Rapidly rotating turbulent rayleigh-benard convections. *J. Fluid Mech.*, 332, 1996.
- M. K.-H Kiessling and T. Neukirch. Negative specific heat of a magnetically self-confined plasma torus. *PNAS*, 100:1510–1514, 2003.
- A. S. Kingsep, K. V. Chukbar, and V. V. Yankov. *Reviews of Plasma Physics*, volume 16, page 1. Consultants Bureau, New York, 1989.
- R. Kinney, T. Tajima, and N. Petviashvili. Discrete vortex representation of magnetohydrodynamics. *Phys. Rev. Lett.*, 71:1712–1715, 1993.

- R. Klein and A. J. Majda. Self-stretching of a perturbed vortex filament i: The asymptotic equation for deviations from a straight line. *Physica D*, 49:323, 1991.
- R. Klein, A. Majda, and K. Damodaran. Simplified equation for the interaction of nearly parallel vortex filaments. *J. Fluid Mech.*, 288:201–48, 1995.
- A. N. Kolmogorov. Local structure of turbulence in an incompressible fluid at very high Reynolds number. *Dokl. Akad. Nauk SSSR*, 30:299–302, 1941.
- J. W. Lawson. Path integrals for the quantum microcanonical ensemble. *Phys. Rev. E*, 61:61–65, 2000.
- C. C. Lim. Phase transitions to super-rotation in a coupled barotropic fluid - rotating sphere system. Steklov Inst., Moscow, August 2006. Plenary Talk in Proc. IUTAM Symp., Springer-Verlag.
- C. C. Lim and S. M. Assad. Self-containment radius for rotating planar flows, single-signed vortex gas and electron plasma. *R & C Dynamics*, 10:240–54, 2005.
- C. C. Lim and J. Nebus. *Vorticity Statistical Mechanics and Monte-Carlo Simulations*. Springer, New York, 2006.
- P-L. Lions and A. J. Majda. Equilibrium statistical theory for nearly parallel vortex filaments. In *Proc. CPAM*, volume LIII, pages 76–142. CPAM, 2000.
- D. Lynden-Bell and R. M. Lynden-Bell. On the negative specific heat paradox. *Mon. Not. R. astr. Soc.*, 181:405–419, 1977.
- D. Lynden-Bell and R. Wood. The gravo-thermal catastrophe in isothermal spheres and the onset of red-giant structure for stellar systems. *Mon. Not. R. astr. Soc.*, 138:495–525, 1968.
- L. Onsager. Statistical hydrodynamics. *Nuovo Cimento Suppl.*, 6:279–87, 1949.
- E. Schrödinger. *Statistical Thermodynamics*. Cambridge UP, Cambridge, 1952.
- W. Thirring. Systems with negative specific heat. *Z. Phys*, 235:339, 1970.

- L. Ting and R. Klein. *Viscous Vortical Flows*, volume 374 of *Lecture Notes in Physics*. Springer, Berlin, 1991.
- L. Uby, M. B. Isichenko, and V. V. Yankov. Vortex filament dynamics in plasmas and superconductors. *Phys. Rev. E*, 52:932–939, 1995.
- H. J. Van Leeuwen. Problèmes de la théorie électronique du magnétisme. *J. Phys. Radium*, 6:361, 1921.
- A. Zee. *Quantum Field Theory in a Nutshell*. Princeton UP, Princeton, 2003.

APPENDIX A

Evaluating the Free Energy Integral

In this section we discuss our evaluation of the integral

$$f[i\tau] = -\log \left[\int D\psi \exp(S) \right], \quad (\text{A.1})$$

where

$$S = \left[\beta' L \log(R^2)/4 - \frac{1}{2} \int_0^L d\sigma \alpha' \beta' \left| \frac{\partial \psi(\sigma)}{\partial \sigma} \right|^2 + (i\tau + 2\mu) |\psi(\sigma)|^2 - iR^2 \tau \right], \quad (\text{A.2})$$

$\beta' = \beta N$, and $\alpha' = \alpha N^{-1}$.

The free-energy, Equation A.1, involves a simple harmonic oscillator with a constant external force, and we can re-write it,

$$f[i\tau] = -\frac{1}{2} i\tau L R^2 - \beta' L \log(R^2)/4 - \ln h[i\tau]. \quad (\text{A.3})$$

Here h is the partition function for a quantum harmonic oscillator in imaginary time,

$$h[i\tau] = \int D\psi \exp \left(\int_0^L d\sigma - \frac{1}{2} m [|\partial_\sigma \psi|^2 + \omega^2 |\psi|^2] \right), \quad (\text{A.4})$$

which has the well-known solution for periodic paths in (2+1)-D where we have integrated the end-points over the whole plane as well,

$$h[i\tau] = \frac{e^{-\omega L}}{(e^{-\omega L} - 1)^2}, \quad (\text{A.5})$$

where $m = \alpha' \beta'$ and $\omega^2 = (i\tau + 2\mu)/(\alpha' \beta')$ (Brown [1992], Zee [2003]).

Let us make a change of variables $\lambda = i\tau + 2\mu$. Then the free-energy reads

$$f[\lambda] = \left(\mu - \frac{1}{2} \lambda \right) L R^2 - \beta' L \log(R^2)/4 - \ln \frac{e^{-\omega L}}{(e^{-\omega L} - 1)^2}, \quad (\text{A.6})$$

where $\omega = \sqrt{\lambda/(\alpha' \beta')}$.

APPENDIX B

Source Code

```
program FKPIMC

c aug. 14th, 2005
c Purpose: Runs PIMC algorithm for nearly parallel vortex filaments
c of Klein/Majda.
c Loops until statistical equilibrium is reached and then begins
c collecting statistical data on the filaments.

c Outputs: energy for each timestep until equilibrium, the complete
c configuration at each step after statistical equilibrium is reached.
  implicit none
  integer mdim, mdiv, mnts, mnf, msteps, mstatsteps, mnb, nz,
+ nint, nint0

  parameter (mdim=3,
+ mdiv=10, ! max divisions in the bisection algorithm (number of tree levels)
+ mnf=50, ! max number of filaments
+ msteps=10**8, ! max number of steps is 100 million
+ mstatsteps=10000000, ! max number of statistics gathering steps is 10000
+ mnb=1+2**mdim) ! max number of beads in each filament

  real r(mnf,mdim,mnb), ! the actual position of the filaments
+ pr(mnf,mdim,mnb), ! the proposed new position of the filaments
+ pPotEn(mnf,mnf,mdiv), ! proposed potential energy
+ potEn(mnf,mnf,mdiv), ! actual potential energy
+ pAngMo(mnf,mdiv), ! proposed angular momentum
+ angMo(mnf,mdiv), ! actual angular momentum
+ pKinEn(mnf,mdiv), ! proposed kinetic energy
+ kinEn(mnf,mdiv), ! actual kinetic energy
+ pEn(mdiv,2), ! the proposed total energy
+ en(mdiv,2), ! actual total energy
+ alpha,
```

```

+beta,
+mu,
+length,
+delta,
+circ,
+prob, lastprob, accFac, movedist,
+ke,pe,am, rad, coin

real randNoZero

integer nfil, ! number of filaments
+nsteps, ! number of monte carlo steps before statistics are gathered
+nstatsteps, ! number of monte carlo accepted steps where stats are gathered
+ndiv, ! number of divisions in bisection algorithm
+nbds, ! number of beads in each filament
+nwcacc, nbsacc, ! number of accepted steps
+seed, i, j, k, l, istep, ntotsteps,
+whichfil,
+nwcprob1, nbsprob1, lastacc,
+fil(2),
+now(3),
+start(3),
+elapsed

character charbuf*100, ofname*100, enfname*100, infname*100

write (*,*) ' Author: Timothy Andersen'

! read in command line arguments:
! output file
if (iargc().ge.13) then
  call getarg(1,charbuf)
  read (charbuf,*) alpha
  call getarg(2,charbuf)
  read (charbuf,*) beta

```

```

call getarg(3,charbuf)
read (charbuf,*) mu
    call getarg(4,charbuf)
    read (charbuf,*) circ
call getarg(5,charbuf)
read (charbuf,*) length
call getarg(6,charbuf)
read (charbuf,*) ndiv
call getarg(7,charbuf)
read (charbuf,*) nfil
call getarg(8,charbuf)
read (charbuf,*) nsteps
call getarg(9,charbuf)
read (charbuf,*) nstatsteps
call getarg(10,charbuf)
read (charbuf,*) movedist
call getarg(11,charbuf)
read (charbuf,*) seed
call getarg(12,ofname)
call getarg(13,enfname)
else
    write(*,*) 'usage: pimc alpha beta mu circ length ndiv
+nfil nsteps '
    write(*,*) 'nstatsteps movedist seed pathout energyout '
    write(*,*) '[inputfile]'
    stop
endif

nbds = 2**ndiv+1
if (ndiv.gt.mdiv) then
    write(*,*) 'error: ndiv=',ndiv,' must be < ',mdiv
    stop
endif
if (alpha.le.0.) then
    write(*,*) 'error: alpha=',alpha,' must be > 0'
    stop
endif
if (mu.le.0.) then

```

```

write(*,*) 'error: mu=',mu,' must be > ',0
stop
endif
if (nfil.gt.mnf) then
write(*,*) 'error: nfil=',nfil,' must be < ',mnf
stop
endif
if (nsteps.gt.msteps) then
write(*,*) 'error: nsteps=',nsteps,' must be < ',msteps
stop
endif
if (nstatsteps.gt.mstatsteps) then
write(*,*) 'error: nstatsteps=',nstatsteps,' must be < ',
+ mstatsteps
stop
endif
if (movedist.lt.0.) then
write(*,*) 'error: movedist=',movedist,' must be < 0'
stop
endif

write(*,*) 'beta=',beta
write(*,*) 'mu=',mu
write(*,*) 'alpha=',alpha
write(*,*) 'length=',length
write(*,*) 'N=',nfil
write(*,*) 'circ=',circ
call srand (seed)

if (iargc().ge.14) then
call getarg(14,infname)
call loadpos(r,mnf,mnb,nfil,mdim,nbds,length,infname)
else
call initpos(r,mnf,mnb,nfil,mdim,nbds,length,mu)
endif

! initialize the proposed position
do 120 k=1,mnb

```

```

do 120 j=1,mdim
do 120 i=1,mnf
pr(i,j,k) = r(i,j,k)
120 continue
open(1,file=ofname,status='unknown',form='formatted')
write(1,*) nfil,nbds
call printConfig(r,en,mnf,mnb,mdiv,nfil,mdim,nbds,ndiv,0,0)

do l=1,mdiv
do i=1,mnf
angMo(i,l) = 0.
pAngMo(i,l) = 0.
kinEn(i,l) = 0.
pKinEn(i,l) = 0.
do j=1,mnf
potEn(i,j,l) = 0.
pPotEn(i,j,l) = 0.
enddo
enddo
enddo

! initialize the energies
delta=length
do l=1,ndiv
delta=delta/2.
fil(1) = 1
fil(2) = nfil

call potEnergy(potEn,potEn,pr,mnf,mnb,mdiv,nfil,mdim,nbds,ndiv
+,fil,l,delta)
call angMoment(angMo,angMo,pr,mnf,mnb,mdiv,nfil,mdim,nbds,ndiv
+,fil,l,delta)
call kineticEnergy(kinEn,kinEn,pr,mnf,mnb,mdiv,nfil,mdim,nbds
+,ndiv,fil,l,delta)

call totalEnergy(en,potEn,angMo,kinEn,mu,beta,alpha,circ,
+mnf,mdiv,
+nfil,ndiv,l)

```

```

        pEn(1,1) = en(1,1)
        pEn(1,2) = en(1,2)
    enddo

    nwcacc = 0
    nbsacc = 0
    nwcprob1 = 0
    nbsprob1 = 0
    lastacc = 0
    ntotsteps = nsteps+nstatsteps
c    write(enfname,*) 'energy',alpha,'_',beta,'_',mu,'_',nfil,'.out'
c    write(*,*) enfname
    open(2,file=enfname,status='unknown',form='formatted')
c    call itime(start)
    whichfil = 1
    do istep=1,ntotsteps
l=1
delta=length
prob=1.
lastprob=1.
nint=1
        coin = randNoZero()
c    write(*,*) coin
        if (mod(istep,2).ne.0) then
            whichfil = whichfil+1
            if (whichfil.gt.nfil) whichfil = 1
c            write(*,*) whichfil
            fil(1) = whichfil
            fil(2) = whichfil
            do i=fil(1),fil(2)
                call moveendpt(pr,accFac,i,mnf,mnb,nfil,mdim,nbds,
+ movedist,length/(nbds-1),mu,beta,alpha)
            enddo
            ! this is a while loop, it checks to see if a rejection
            ! or acceptance is made.
150    if (randNoZero().lt.prob.and.1.le.ndiv) then
                delta = delta/2.
                    call getSystemProb(pr,en,pEn,potEn,pPotEn,kinEn

```

```

+,pKinEn,fil,angMo,pAngMo,
+mnf,mnb,mdim,mdiv,nfil,nbds,ndiv,beta,alpha,mu,circ,length,
+prob,lastprob,l,delta,accFac,1)

        l = l + 1
        goto 150
    endif
    lastacc = nwcacc
    call accOrRejMove(r,pr,en,pEn,potEn,pPotEn,kinEn,pKinEn,
+angMo,pAngMo,fil,mnf,mnb,mdim,mdiv,nfil,nbds,ndiv,istep,nsteps,
+prob,nwcacc,nwcprob1,l,whichfil,1)
        lastacc = nwcacc - lastacc
    else
        ! this is a while loop, it checks to see if a rejection
        ! or acceptance is made.
c        write(*,*) whichfil

        fil(1) = whichfil
        fil(2) = whichfil
180    if (randNoZero().lt.prob.and.l.le.ndiv) then
        delta = delta/2.

        call bsect(pr,mnf,mnb,ndiv,nfil,mdim,nbds,beta,alpha,
+mu,circ,l,delta,fil,movedist,length)
    call getSystemProb(pr,en,pEn,potEn,pPotEn,kinEn,pKinEn,
+fil,angMo,pAngMo,
+mnf,mnb,mdim,mdiv,nfil,nbds,ndiv,beta,alpha,mu,circ,length,
+prob,lastprob,l,delta,1.,2)

        l = l + 1
        goto 180
    endif
    lastacc = nbsacc
    call accOrRejMove(r,pr,en,pEn,potEn,pPotEn,kinEn,pKinEn,
+    angMo,pAngMo,fil,
+ mnf,mnb,mdim,mdiv,nfil,nbds,ndiv,istep,nsteps,
+ prob,nbsacc,nbsprob1,l,whichfil,2)
    lastacc = nbsacc - lastacc

```

```

endif
if (mod(istep,100).eq.0) then
c   call itime(now)
c   elapsed = (now(1)-start(1))*3600 + (now(2)-start(2))*60 +
c   + (now(3) - start(3))
      pe = 0.
      ke = 0.
      am = 0.
      do i=1,mnf
        do j=1,mnf
          pe = pe + circ*circ*beta*potEn(i,j,ndiv)
        enddo
        ke = ke + alpha*beta*kinEn(i,ndiv)
        am = am + circ*mu*angMo(i,ndiv)
      enddo
      write (2,200) istep,pe,ke,am,beta*en(ndiv,1),beta*en(ndiv,2)
endif
200  format(i10,5(e14.5))

enddo
call printConfig(r,en,mnf,mnb,mdiv,nfil,mdim,nbds,ndiv,istep,
+whichfil)
write(*,*) 'No. Wholechain Steps Accepted: ', nwcacc
write(*,*) 'No. Wholechain Prob. 1 Moves: ', nwcprob1
      write(*,*) 'No. Bisect Steps Accepted: ', nbsacc
write(*,*) 'No. Bisect Prob. 1 Moves: ', nbsprob1

close(1)
close(2)

end
!!!!!!!!!!!!!!!!!!!!!!!!!!!!!!!!!!!!!!!!!!!!!!!!!!!!!!!!!!!!!!!!!!!!!!!!!!!!!!
! this routine loads the positions of the filaments in (x,y) space !
!!!!!!!!!!!!!!!!!!!!!!!!!!!!!!!!!!!!!!!!!!!!!!!!!!!!!!!!!!!!!!!!!!!!!!!!!!!!!!
subroutine loadpos(r,mnf,mnb,nfil,mdim,nbds,length,infname)
implicit none
integer mnf,mnb,mdim,nfil, nbds, i, k, n, j, nfil0,nbds0,fil0
real r(mnf,mdim,mnb), length, delta, mu, u1,u2,dy,dx,sigmasq

```

```

character infname*100
delta = length/(nbds-1)
open(3,file=infname,status='unknown',form='formatted')
read(3,*) nfil0,nbds0
if (nfil0.ne.nfil) then
    write(*,*) 'error: incorrect input file format'
    stop
elseif (nbds0.ne.nbds) then
    write(*,*) 'error: incorrect input file format'
    stop
endif
do n=1,2
do i=1,nfil
    read(3,*) fil0
do k=1,nbds
    read(3,350) (r(i,j,k),j=1,mdim-1)
    r(i,3,k) = (k-1)*delta
c    write(*,*) n,i,k,(r(i,j,k),j=1,mdim-1)
enddo
enddo
enddo
350 format(2(e14.5))
close(3)
end

!!!!!!!!!!!!!!!!!!!!!!!!!!!!!!!!!!!!!!!!!!!!!!!!!!!!!!!!!!!!!!!!!!!!!!!!!!!!!!
! this routine initializes the positions of the filaments in (x,y) space !
!!!!!!!!!!!!!!!!!!!!!!!!!!!!!!!!!!!!!!!!!!!!!!!!!!!!!!!!!!!!!!!!!!!!!!!!!!!!!!
subroutine initpos(r,mnf,mnb,nfil,mdim,nbds,length,mu)
implicit none
integer mnf,mnb,mdim,nfil, nbds, i, k
real r(mnf,mdim,mnb), length, delta, mu, u1,u2,dy,dx,sigmasq,
+randNoZero

delta = length/(nbds-1)
c    sigmasq = 1./(2*length*mu)

do i=1,nfil

```

```

c      u1 = randNoZero()
c      u2 = randNoZero()

c      dx = cos(2.d0*3.14159265357d0*u1)
c      + *sqrt(-2*sigmasq*log(u2))
c      dy = sin(2.d0*3.14159265357d0*u1)
c      + *sqrt(-2*sigmasq*log(u2))
c      dx = 0.2*randNoZero() - 0.1
c      dy = 0.2*randNoZero() - 0.1
c      r(i,1,1) = dx
c      r(i,2,1) = dy
c      r(i,3,1) = 0.
c      write(*,*) rad,r(i,1,k),r(i,2,k)
do k=2,nbds
c      r(i,1,k) = r(i,1,1)
c      r(i,2,k) = r(i,2,1)
c      r(i,3,k) = (k-1)*delta
enddo
enddo
end

! Accepts the configuration by copying the information from the temporary
! data structures into the permanent ones.
subroutine acceptConfig(r,en,kinEn,angMo,potEn,pr,pEn,pKinEn,
+      pAngMo, pPotEn, fil,mnf,mdim,mnb,nfil,nbds,ndiv,mdiv)
implicit none
integer whichfil, nfil, mdim, nbds, ndiv, mdiv, i, j, k, l,
+ mnf, mnb, fil(2)
real r(mnf,mdim,mnb), ! the actual position of the filaments
+pr(mnf,mdim,mnb), ! the proposed new position of the filaments
+pPotEn(mnf,mnf,mdiv), ! proposed potential energy
+potEn(mnf,mnf,mdiv), ! actual potential energy
+pAngMo(mnf,mdiv), ! proposed angular momentum
+angMo(mnf,mdiv), ! actual angular momentum
+pKinEn(mnf,mdiv), ! proposed kinetic energy
+kinEn(mnf,mdiv), ! actual kinetic energy

```

```

+pEn(mdiv,2), ! the proposed total energy
+en(mdiv,2) ! actual total energy

! copy over the old to the new
do l=1,ndiv
  en(l,1) = pEn(l,1)
  en(l,2) = pEn(l,2)
  do i=1,nfil
c    write (*,*) 'a:',i,l,angMo(i,l), pAngMo(i,l)
    angMo(i,l) = pAngMo(i,l)
    kinEn(i,l) = pKinEn(i,l)
c    write (*,*) 'kinEn=',kinEn(i,l)
    do j=i+1,nfil
      potEn(i,j,l) = pPotEn(i,j,l)
c    potEn(j,whichfil,l) = pPotEn(j,whichfil,l)
c    write (*,*) 'potEn=',potEn(i,j,l)
    enddo
  enddo
  do 100 i=1,nfil
    do 100 j=1,mdim
      do 100 k=1,nbds
r(i,j,k) = pr(i,j,k)
100 continue
  end

  subroutine printConfig(r,en,mnf,mnb,mdiv,nfil,mdim,nbds,ndiv,step,
+whichfil)
  implicit none
  integer nfil, mdim, nbds, ndiv, step, i, j, k,mnf,mnb,mdiv,fst,
+lst,whichfil
  real r(mnf,mdim,mnb), ! the actual position of the filaments
+en(mdiv,2) ! actual total energy

c  write (1,*) step
  if (whichfil.eq.0) then
    fst = 1

```

```

        lst = nfil
    else
        fst = whichfil
        lst = whichfil
    endif

    do i=fst,lst
c       write(*,*) i,fst,lst,whichfil,nbds
        write (1,*) i
c       write (1,290) (r(i,j,1),j=1,mdim)
        do k=1,nbds
            write(1,290) (r(i,j,k),j=1,mdim-1)
        enddo
        enddo
290    format(2(e14.5))

    end

    subroutine potEnergy(pPotEn,potEn,pr,mnf,mnb,mdiv,nfil,mdim,nbds,
+ ndiv,fil,l,delta)
    implicit none
    integer mnf,mnb,mdiv,nfil, i,j,k,l,n,mdim,nbds,ndiv,inc,
+ m,fil(2)
    real pPotEn(mnf,mnf,mdiv),
+potEn(mnf,mnf,mdiv),
+pr(mnf,mdim,mnb),
+delta, d

    inc = 2**(ndiv-1)
c       write(*,*) inc, whichfil
        do i=1,nfil
            do j=i+1,nfil
c if either index corresponds to a particle that has changed,
c recalculate the potential energy, otherwise use the old value
                if ((i.ge.fil(1).and.i.le.fil(2))
+ .or.(j.ge.fil(1).and.j.le.fil(2))) then
                    ! skip over the beads that are not used in this level
c                 m=0

```

```

c      write(*,*) i,j,l,pPotEn(i,j,l)
          pPotEn(i,j,l) = 0.
do k=1,(nbds-1),inc
d = (pr(i,1,k)-pr(j,1,k))**2 + (pr(i,2,k)-pr(j,2,k))**2
          if (d.gt.0) then
              pPotEn(i,j,l) = -delta*0.5*log(d) + pPotEn(i,j,l)
          endif
c      write(*,*) i,j,l,pPotEn(i,j,l)
c m = m + 1
      enddo
c      write(*,*) m,nbds,inc
      else
          pPotEn(i,j,l) = potEn(i,j,l)
      endif
c      write(*,*) i,j,fil(1),l,pPotEn(i,j,l),potEn(i,j,l)
      enddo
      enddo

      end

      subroutine angMoment(pAngMo,angMo,pr,mnf,mnb,mdiv,nfil,mdim,nbds,
+ ndiv,fil,l,delta)
      implicit none
      integer mnf,mnb,mdiv,nfil, ndiv, nbds, l, i, j, k,
+ n, mdim, inc, fil(2)
      real pAngMo(mnf,mdiv), ! proposed angular momentum
+angMo(mnf,mdiv),
+pr(mnf,mdim,mnb), delta, dsq

      inc = 2**(ndiv-1)
      do i=1,nfil
          if (i.ge.fil(1).and.i.le.fil(2)) then
              ! reuse the previous level
if (l.gt.1) then
pAngMo(i,l) = pAngMo(i,l-1)/2.
else
          dsq = pr(i,1,1)**2 + pr(i,2,1)**2
          pAngMo(i,1) = delta*dsq

```

```

endif
    do k=inc+1,(nbds-1),2*inc
        dsq = pr(i,1,k)**2 + pr(i,2,k)**2
        pAngMo(i,l) = delta*dsq + pAngMo(i,l)
    enddo
c    write(*,*) i,l,pAngMo(i,l)
    else
c write(*,*) i,l,pAngMo(i,l),angMo(i,l)
    pAngMo(i,l) = angMo(i,l)
    endif
enddo
end

subroutine kineticEnergy(pKinEn,kinEn,pr,mnf,mnb,mdiv,nfil,
+ mdim,nbds,ndiv,fil,l,delta)
    implicit none
    integer mnf,mnb,mdiv,nfil, ndiv, nbds, l, i, j, k, n,
+ mdim, inc, fil(2)
    real pKinEn(mnf,mdiv),
+kinEn(mnf,mdiv),
+pr(mnf,mdim,mnb), delta, dsq

    inc = 2**(ndiv-1)
    do i=1,nfil
        if (i.ge.fil(1).and.i.le.fil(2)) then
            do k=1,(nbds-1),inc
                dsq = 0.
                do n=1,(mdim-1)
                    dsq = (pr(i,n,k)-pr(i,n,k+1))**2 + dsq
                enddo
                pKinEn(i,l) = dsq/delta/2.
            enddo
        else
            pKinEn(i,l) = kinEn(i,l)
        endif
    enddo
end

```

```

subroutine totalEnergy(pEn,pPotEn,pAngMo,pKinEn,mu,beta,
+ alpha,circ,mnf,mdiv,nfil,ndiv,lev)
  implicit none
  integer mnf,mdiv,nfil, ndiv, lev, i, j
  real pPotEn(mnf,mnf,mdiv), ! proposed potential energy
+pAngMo(mnf,mdiv), ! proposed angular momentum
+pKinEn(mnf,mdiv),
+pEn(mdiv,2), beta, mu,alpha, pot, kin, ang, circ

  pEn(lev,1) = 0.
  pEn(lev,2) = 0.
  pot = 0.
  kin = 0.
  ang = 0.
  do i=1,nfil
    do j=i+1,nfil
      pot = circ*circ*pPotEn(i,j,lev) + pot
c      write(*,*) pPotEn(i,j,lev)
    enddo
      ang = circ*pAngMo(i,lev)*mu/beta + ang
c      kin = alpha*pKinEn(i,lev) + kin
c      write(*,*) i,lev,pAngMo(i,lev),pKinEn(i,lev), pEn(lev,1)
    enddo
c we don't include them because angular momentum and kinetic energy
c are being sampled
      pEn(lev,1) = pot + ang
      pEn(lev,2) = pot
c      write(*,*) lev,pot,ang,kin,pEn(lev,1),pEn(lev,2)
    end

subroutine moveendpt(pr,accFac,whichfil,mnf,mnb,nfil,mdim,nbds,
+ movedist,delta,mu,beta,alpha)
  implicit none
  integer whichfil, mnf,mnb,nfil, mdim, nbds, k
  real pr(mnf,mdim,mnb), movedist, dx, dy, u1, u2
+, dr, darc, dth, rad, accFac, th, sigmasq, mu, delta,
+ beta, alpha, randNoZero

```

```

accFac = 1.
c   sigmasq = 1./(2*delta*mu)
c   u1 = randNoZero()
c   u2 = randNoZero()

c   dx = cos(2.d0*3.14159265357d0*u1)
c   + *sqrt(-2*sigmasq*log(u2))
c   dy = sin(2.d0*3.14159265357d0*u1)
c   + *sqrt(-2*sigmasq*log(u2))
c   dx = dx - pr(whichfil,1,1)
c   dy = dy - pr(whichfil,2,1)
c   write(*,*) dx, dy, dr, darc
dx = 2.*movedist*randNoZero() - movedist
dy = 2.*movedist*randNoZero() - movedist
c   write(*,*) dx, dy

do k=1,nbds
c   pr(whichfil,1,1) = alpha*beta/delta*sigmasq*
c   + (pr(whichfil,1,nbds-1)+pr(whichfil,1,2)) + dx
c   pr(whichfil,2,1) = alpha*beta/delta*sigmasq*
c   + (pr(whichfil,2,nbds-1)+pr(whichfil,2,2)) + dy
c   pr(whichfil,1,nbds) = pr(whichfil,1,1)
c   pr(whichfil,2,nbds) = pr(whichfil,2,1)
c   pr(whichfil,1,k) = pr(whichfil,1,k) + dx
c   pr(whichfil,2,k) = pr(whichfil,2,k) + dy
enddo

end

subroutine accOrRejMove(r,pr,en,pEn,potEn,pPotEn,kinEn,pKinEn,
+ angMo,pAngMo,fil,
+ mnf,mnb,mdim,mdiv,nfil,nbds,ndiv,istep,nsteps,
+ prob,nacc,nprob1,l,whichfil,mv)
implicit none
integer mnf,mnb,mdim,mdiv,nfil,nbds,ndiv,l,nacc,nprob1,whichfil,
+ istep, nsteps, k, j, i, fil(2), first, mv
save first
data first /1/

```

```

    real r(mnf,mdim,mnb),
+ pr(mnf,mdim,mnb),
+ en(mdiv,2),
+ pEn(mdiv,2),
+ potEn(mnf,mnf,mdiv),
+ pPotEn(mnf,mnf,mdiv),
+ kinEn(mnf,mdiv),
+ pKinEn(mnf,mdiv),
+ angMo(mnf,mdiv),
+ pAngMo(mnf,mdiv),
+ beta, alpha, mu, length, delta, prob, lastprob, randNoZero

    if (istep.ge.nsteps.and.first.eq.1) then
c print out full config for first one and changes only thereafter
        call printConfig(r,en,mnf,mnb,mdiv,nfil,mdim,nbds,ndiv,istep,
+0)
        first = 0
    endif

    ! if we have an acceptance
    if (randNoZero().lt.prob.and.l.gt.ndiv) then
        call acceptConfig(r,en,kinEn,angMo,potEn,pr,pEn,pKinEn,
+ pAngMo, pPotEn, fil,mnf,mdim,mnb,nfil,nbds,
+ ndiv,mdiv)
        if (istep.ge.nsteps.and.first.eq.0) then
            call printConfig(r,en,mnf,mnb,mdiv,nfil,mdim,nbds,ndiv,
+istep,whichfil)
        endif

        nacc = nacc + 1
        if (prob.eq.1.) nprob1 = nprob1 + 1

        ! if we're in the stats. collecting stage (istep>nsteps)
    else
c        write(*,*) 'R:',fil(1),pEn(ndiv),en(ndiv)
        do 220 k=1,mnb
        do 220 j=1,mdim
        do 220 i=1,mnf

```

```

pr(i,j,k) = r(i,j,k)
220  continue
    endif

end

subroutine getSystemProb(pr,en,pEn,potEn,pPotEn,kinEn,pKinEn,
+ fil, angMo, pAngMo,
+ mnf,mnb,mdim,mdiv,nfil,nbds,ndiv,beta,alpha,mu,circ,length,
+ prob,lastprob,l,delta,accFac,mv)
  implicit none
  integer mnf,mnb,mdim,mdiv,nfil,nbds,ndiv,l,fil(2), mv
  real pr(mnf,mdim,mnb),
+ potEn(mnf,mnf,mdiv),
+ pPotEn(mnf,mnf,mdiv),
+ kinEn(mnf,mdiv),
+ pKinEn(mnf,mdiv),
+ angMo(mnf,mdiv),
+ pAngMo(mnf,mdiv),
+ en(mdiv,2),
+ pEn(mdiv,2),
+ beta, alpha, mu, length, delta, prob, lastprob, accFac, circ

  call potEnergy(pPotEn,potEn,pr,mnf,mnb,mdiv,nfil,mdim,nbds,ndiv,
+ fil,l,delta)
  call angMoment(pAngMo,angMo,pr,mnf,mnb,mdiv,nfil,mdim,nbds,ndiv,
+ fil,l,delta)
  call kineticEnergy(pKinEn,kinEn,pr,mnf,mnb,mdiv,nfil,mdim,nbds,
+ ndiv,fil,l,delta)

  call totalEnergy(pEn,pPotEn,pAngMo,pKinEn,mu,beta,alpha,circ,mnf,
+ mdiv,nfil,ndiv,l)

  ! test for acceptance at each level
  if (pEn(l,mv).le.en(l,mv)) then
    prob=1.
  else

```

```

        prob = accFac*exp(-beta*(pEn(l,mv)-en(l,mv)))/lastprob
    endif

c        if (prob.gt.0) then
c    write(*,*) l,mv,beta*pEn(l,mv), beta*en(l,mv),prob,lastprob
c        endif
        lastprob=prob
    end

subroutine bsect(pr,mnf,mnb,ndiv,nfil,mdim,nbds,beta,alpha,
    + mu,circ,l,delta,fil,movedist,length)
implicit none
integer mnf,mnb,mdim,ndiv,nfil,nbds,l,inc,k,i,fil(2)

    real pr(mnf,mdim,mnb),beta,alpha,delta,u1,u2,dx,dy,sigmasq,
    +movedist,mu,delta2,length, randNoZero, circ

inc = 2**(ndiv-1)
    delta2 = length/(nbds-1)
sigmasq = 1/(2*alpha*beta/delta + 2*circ*mu*delta2)
do k=inc+1,(nbds-1),2*inc
do i=fil(1),fil(2)
        pr(i,3,k)=.5d0*(pr(i,3,k-inc)+pr(i,3,k+inc))
        u1 = randNoZero()
650    u2 = randNoZero()
        if (u2.eq.0) then
            goto 650
        endif

        dx = cos(2.d0*3.14159265357d0*u1)
    + *sqrt(-2*sigmasq*log(u2))
        dy = sin(2.d0*3.14159265357d0*u1)
    + *sqrt(-2*sigmasq*log(u2))

        pr(i,1,k)=dx + alpha*beta/delta*sigmasq*
    +(pr(i,1,k-inc)+pr(i,1,k+inc))
        pr(i,2,k)=dy + alpha*beta/delta*sigmasq*
    +(pr(i,2,k-inc)+pr(i,2,k+inc))

```

```
c      pr(i,1,k)=pr(i,1,k) + randNoZero()*2*movedist - movedist
c      pr(i,2,k)=pr(i,2,k) + randNoZero()*2*movedist - movedist
c      if (l.eq.ndiv) write(*,*) i,k,l,pr(i,1,k),pr(i,2,k),pr(i,3,k)
      enddo
      enddo
      end

      real function randNoZero()
      real x
700  x = rand()
      if (x.gt.0) then
          randNoZero=x
      else
          goto 700
      endif
      return
      end
```